Analysis of Chattering in Systems With Second-Order Sliding Modes

Igor Boiko, *Member, IEEE*, Leonid Fridman, *Member, IEEE*, Alessandro Pisano, *Member, IEEE*, and Elio Usai, *Member, IEEE*

***Abstract*—A systematic approach to the chattering analysis in systems with second-order sliding modes is developed. The neglected actuator dynamics is considered to be the main cause of chattering in real systems. The magnitude of oscillations in nonlinear systems with unmodeled fast nonlinear actuators driven by second-order sliding-mode control generalized suboptimal (2-SMC G-SO) algorithms is evaluated. Sufficient conditions for the existence of orbitally stable periodic motions are found in terms of the properties of corresponding Poincaré maps. For linear systems driven by 2-SMC G-SO algorithms, analysis tools based on the frequency-domain methods are developed. The first of these techniques is based on the describing function method and provides for a simple approximate approach to evaluate the frequency and the amplitude of possible periodic motions. The second technique represents a modified Tsypkin's method and provides for a relatively simple, theoretically exact, approach to evaluate the periodic motion parameters. Examples of analysis and simulation results are given throughout this paper.**

***Index Terms*—Frequency-domain methods, limit cycles, Poincaré map analysis, sliding-mode control.**

I. Introduction

THE sliding-mode control (SMC) approach was developed in the late 1950s [42], and by the end of the 1970s, it was recognized as one of most promising robust control techniques [25], [38], [39], [17], [41].

However, the very first implementations of the SMC technique showed that the real sliding mode exhibited chattering, which appears to be the most problematic issue in SMC applications [44].

The following three main approaches to chattering elimination and attenuation in SMC systems were proposed in the mid-1980s.

Manuscript received July 18, 2006; revised February 1, 2007 and March 13, 2007. Recommended by Associate Editor S. Celikovsky. This work was supported in part by the Mexican CONACyT (Consejo Nacional de Ciencia y Tecnologia) under Grants 43807-Y and J110.418/2006, the Programa de Apoyo a Proyectos de Investigacion e Innovacion Tecnolgica (PAPIIT) UNAM under Grant 107006-2, and the Italian MURST Project "Novel control systems in high-speed railways."

I. Boiko is with the Department of Electrical and Computer Engineering, University of Calgary, Calgary, AB T2N 1N4 Canada (e-mail: i.boiko@ieee.org).

L. Fridman is with the Department of Control, Engineering Faculty, National Autonomous University of Mexico (UNAM), 04510, Mexico, D.F., Mexico (e-mail: lfridman@servidor.unam.mx).

A. Pisano and E. Usai are with the Department of Electrical and Electronic Engineering (DIEE), University of Cagliari, 09123 Cagliari, Italy (e-mail: pisano@diee.unica.it; eusai@diee.unica.it).

Color versions of one or more of the figures in this paper are available online at http://ieeexplore.ieee.org.

Digital Object Identifier 10.1109/TAC.2007.908319

— The use of the *saturation control* instead of the discontinuous one [14], [36]. This approach allows for the control continuity but cannot restrict the system dynamics onto the switching surface. It only ensures the convergence to a boundary layer of the sliding manifold whose size is defined by the slope of the saturation characteristics.

— *The observer-based approach* [13], [41]. This method allows for bypassing the plant dynamics by the chattering loop. This approach reduces the problem of robust control to the problem of exact robust estimation and, consequently, can lead to the deterioration of robustness with respect to the plant uncertainties due to the mismatch between the observer and plant dynamics [44].

— *The high-order sliding-mode approach* [18], [26]. It allows for finite-time convergence to zero of not only the so-called sliding variable but its derivatives too. This approach was actively developed over the last two decades [4], [6], [7], [5], [26], [27], [30], [23], [34] as not only means of chattering attenuation but also as means of robust control of plants of relative degree two and higher. Theoretically, rth-order sliding modes would totally suppress chattering in the *model of the system* (but not in the actual system) when the relative degree of the *model* of the plant (including actuators and sensors) is r. Yet, no model can fully account for parasitic dynamics and, consequently, the chattering effect cannot be avoided.

There are different approaches to analysis of chattering that take into account different causes of chattering: the presence of fast actuators and sensors [40], [20], [22], [42], [9] and the existence of time delay and hysteresis [43], [3], [40], [41]. There also may be other causes of chattering: the effect of quantization (see, for example, [28]) and a bifurcation of the system behavior (see [8] and bibliography therein).

The purpose of this paper is to develop a systematic approach to the chattering analysis in control systems with second-order sliding-mode controllers (2-SMC) caused by the *presence of fast actuators*.

A. Methodology of Analysis

There exist two approaches to analysis of fast oscillations caused by the presence of fast actuators: the time-domain approach, which is based on the state–space representation, and the frequency-domain approach.

The estimation of the oscillation magnitude in standard (i.e., first-order) SMC systems with fast actuators and sensors was developed in [40], [21], and [22] via the combined use of the singularly perturbed relay control systems theory and the Lyapunov techniques. However, the Lyapunov theory is not easily applicable to the description of the finite-time convergence properties of 2-SMC system, and the trajectories generated by 2-SMC algorithms are much more complicated than those generated by the first-order SMC, thereby requiring new decomposition and estimation techniques.

The Poincaré maps are successfully used for analysis of periodic oscillations in the relay control systems (see, for example, [31] and [16]). In [20], a decomposition of Poincaré maps was proposed to analyze chattering in systems with first-order sliding modes, which led to Pontryagin–Rodygin-like [32] averaging theorems. Such theorems provide sufficient conditions for the existence and stability of fast periodic motions.

The describing function (DF) method [2] offers finding approximate values of the frequency and the amplitude of periodic motions in systems with linear plants driven by the sliding-mode controllers [45], [33]. The Tsypkin locus [43] provides an exact solution of the periodic problem, including finding exact values of the amplitude and the frequency of the steady-state oscillation. The aforementioned frequency-domain methods were developed to analyze relay feedback systems and cannot be used directly for the analysis of 2-SMC systems. In [10] and [11], the DF method was adapted to analysis of the twisting and the super-twisting 2-SMC algorithms [26]. In [12], a DF-based method of parameter adjustment of the generalized suboptimal (G-SO) 2-SMC algorithm [5], [7] was proposed to ensure the desired frequency and amplitude of the periodic oscillation (chattering).

B. Main Contribution

In this paper, a systematic approach to analysis of chattering in 2-SMC systems is developed. The presence of parasitic dynamics is considered to be the main cause of chattering, and the respective effects are analyzed by means of a few techniques. The treatment is developed by considering the G-SO algorithm [5], [7]. The main results could be easily generalized to the twisting algorithm [26] with minor modifications in the proofs.

For a class of nonlinear uncertain systems with nonlinear fast actuators, the following holds.

1) It is proved that the approximability domain [29], [46] of the 2-SMC G-SO algorithms depends on the actuator time constant μ as $O(\mu^2)$ and $O(\mu)$ for the sliding 2-SMC variable and its derivative, respectively. Next, results concerning the detailed analysis of the chattering trajectories are obtained via the Poincaré maps and frequency-domain methods, which involve the fullest utilization of the system model.
2) Sufficient conditions of the existence of asymptotically orbitally stable periodic solution are obtained in terms of Poincaré maps.
   For linear, possibly linearized, dynamics driven by 2-SMC G-SO algorithms, frequency-domain methods of analysis of the periodic solutions are developed, and, in particular, the following hold.
3) The describing function method is adapted to perform an approximate analysis of the periodic motions.
4) The Tsypkin's method is modified for the analysis of the systems driven by 2-SMC G-SO algorithms. This modification allows for finding exact values of the parameters of periodic motions, without requiring for the actuator dynamics to be fast.

Remark 1: It is necessary to note here that the problem of chattering in the 2-SMC systems due to the presence of the fast actuators is dual to the problem of the chattering in the 2-SMC systems due to the presence of the fast inertial sensors (see, for example, [22]).

Remark 2: Note that we are not considering here the problem of sliding manifold design.

C. Paper Structure

This paper is organized as follows. In Section II, a class of nonlinear systems with nonlinear fast actuators is introduced. In Section III, we show that the 2-SMC G-SO algorithm with suitably chosen parameters steers the system trajectories in finite time towards an invariant vicinity of the second-order sliding set. We also estimate the amplitude of chattering oscillations as a function of the actuator time constant. In Section IV, sufficient conditions of the existence and stability of fast periodic motions in a vicinity of the second-order sliding set are derived via the Poincaré map approach. In Section V, frequency-domain approaches to chattering analysis are developed. The describing function method is adapted in Section V-A to carry out analysis of periodic motions in systems with linear plants. In Section V-B, the Tsypkin's method is modified to obtain the parameters of the periodic motion exactly. Examples illustrating the application of the proposed methodologies are spread over the paper. The proofs of the theorems are given in Appendices I–V.

II. The 2-SMC Systems With Dynamic Actuators

We will consider a nonlinear single-input system

$$\dot{x} = a(x, z_1) \tag{1}$$

with the state vector $x = [x_1, x_2, \ldots, x_n] \in X \subset R^n$ and the scalar "virtual" control input $z_1 \in Z_1 \subset R$. The plant input z_1 is modifiable via the dynamic fast actuator

$$\mu \dot{z} = h(z, u) \tag{2}$$

where $z = [z_1, z_2, \ldots, z_m] \in Z \subset R^m$ is the actuator state vector, $u \in U \subset R$ is the modifiable actuator input, and $\mu \in R^+$ is a small positive parameter. Let $a : X \times Z_1 \to R^n$ and $h : Z \times U \to R^m$ be vector fields satisfying proper restrictions on their growth and smoothness that will be specified in Section III.

Let the control task for systems (1) and (2) be the finite-time vanishing of the scalar output variable

$$s_1(x) : X \to S_1 \subset R \tag{3}$$

which defines the sliding manifold $s_1(x) = 0$ assigning desired dynamic properties (e.g., stability) to the constrained sliding-mode dynamics. Define

$$s_2(x, z_1) = \frac{\partial s_1(x)}{\partial x} a(x, z_1) : X \times Z_1 \to S_2 \tag{4}$$

and assume that the following conditions hold $\forall (x, z_1) \in X \times Z_1$:

$$\frac{\partial}{\partial z_1} s_2(x, z_1) = 0 \tag{5}$$

$$\frac{\partial}{\partial z_1}\left[\frac{\partial}{\partial x}[s_2(x, z_1)a(x, z_1)]\right] \neq 0. \tag{6}$$

Laborious but straightforward computations show that conditions (5) and (6) hold if and only if

$$\text{rank } J(x, z_1) = 2 \qquad \forall (x, z_1) \in X \times Z_1 \tag{7}$$

with the matrix J defined as follows:

$$J(x, z_1) = \begin{bmatrix} \frac{\partial s_1}{\partial x_1} & \frac{\partial s_1}{\partial x_2} & \cdots & \frac{\partial s_1}{\partial x_n} & 0 \\ \frac{\partial s_2}{\partial x_1} & \frac{\partial s_2}{\partial x_2} & \cdots & \frac{\partial s_2}{\partial x_n} & \frac{\partial s_2}{\partial z_1} \end{bmatrix}. \tag{8}$$

By virtue of the inverse function theorem, one can explicitly define a vector $w \in W \subset \mathbf{R}^{n-2}$ and a diffeomorfic state coordinate change $x = \Phi(s, w) : S \times W \to X$, with $s = [s_1, s_2] \in S$, which is one to one at any point where condition (7) holds [15].

Assume that vector w can be selected in such a way that its dynamics does not depend on the plant input variable z_1, i.e., let the transformed systems (1) and (2) dynamics in the (w, s) coordinates be defined as follows:

$$\dot{w} = g(w, s) \tag{9}$$

$$\dot{s}_1 = s_2 \quad \dot{s}_2 = f(w, s, z_1) \tag{10}$$

$$\mu \dot{z} = h(z, u) \tag{11}$$

where $g : W \times S \to R^{n-2}, f : W \times S \times Z_1 \to R$, and $h : Z \times U \to R^m$ are smooth functions of their arguments such that $f \in \mathbf{C}^2[\bar{W} \times \bar{S} \times \bar{Z}_1]$, $g \in \mathbf{C}^2[\bar{W} \times \bar{S}]$, and $h \in \mathbf{C}^2[\bar{Z} \times \bar{U}]$, where upper bar means the closure of domain.

This means that the "sliding variable" s_1 has a well-defined relative degree $r = 2$ with respect to the plant input variable z_1 over the whole domain of analysis.

We consider the case when the actuator output z_1 has the full relative degree m, equal to the order of the actuator dynamics, with respect to the discontinuous control u.

Remark 3: The special form (9) for the internal dynamics can be always achieved if the original dynamics (1) has affine dependence on z_1 [24]. We are considering in this paper the subclass of nonaffine systems (1) for which such a special choice of vector w can be found.

III. Generalized Suboptimal Algorithm: Convergence Conditions

Consider system (9)–(11) driven by the G-SO 2-SMC algorithm [7]

$$u = -U \text{sign}(s_1 - \beta s_{1Mi}) \tag{12}$$

where U and β are the constant controller parameters and s_{1Mi} is the latest "singular point" of s_1, i.e., the value of s_1 at the most recent time instant $t_{Mi} (i = 1, 2, \ldots)$ such that $\dot{s}_1(t_{Mi}) = 0$. Our analysis is semiglobal in the sense that the initial conditions $w(0), s(0)$, and $z(0)$ are assumed to belong to the known, arbitrarily large, compact domains W_0, S_0, and Z_0, respectively.

The solutions of the system (9)–(12) are understood in the Filippov sense [19].

Remark 4: Since the relative degree between the sliding output s_1 and the discontinuous control u is $m+2$, only sliding modes of order $m+2$, occurring onto the following sliding set[1] [26] can take place

$$s_1 = 0 \tag{13}$$

$$\dot{s}_1 = s_2 = 0 \tag{14}$$

$$\ddot{s}_1(w, 0, z_1) = f(w, 0, z_1) = 0 \tag{15}$$

$$\cdots \tag{16}$$

$$s_1^{(m)}(w, 0, z) = 0 \tag{17}$$

$$s_1^{(m+1)}(w, 0, z) = 0. \tag{18}$$

The internal dynamics in the $(m+2)$-th order sliding-mode is described by[2]

$$\dot{w} = g(w, 0). \tag{19}$$

Suppose that for all $w \in W$ and $z \in Z$ there exists a unique isolated value of $u = u_0(z, w)$ as a solution of equation

$$s_1^{(m+2)}(w, 0, z, u) = 0 \tag{20}$$

which maintains the system trajectories onto the $(m+2)$th-order sliding domain (13)–(18). Note that the actuator input u appears explicitly as an argument of (20), but not of (13)–(18), according to the fact that the relative degree of s_1 with respect to u is $m+2$.

Then, the system equilibrium point can be computed as the unique solution $w_0, z_0, u_0(w_0, z_0)$ of the system of (15)–(20). The knowledge of the equilibrium point will be used in Section V-A to define a local linearization for the system (9)–(11).

Assumption 1: The internal dynamics (9) and the actuator dynamics (11) meet the following input-to-state stability properties for some positive constants ξ_1, ξ_2 [35]

$$\|w(t)\| \leq \|w(0)\| + \xi_1 \sup_{0 \leq \tau \leq t} \|s(\tau)\| \tag{21}$$

$$\|z(t)\| \leq \|z(0)\| + \xi_2 \sup_{0 \leq \tau \leq t} |u(\tau)|. \tag{22}$$

Assumption 2: There exist positive constants H_0, H_1, H_2, G_m, and G_M such that function f is bounded as follows:

$$\begin{aligned} z_1 \leq 0 &: -\tilde{H}(s, w) + G_M z_1 \leq f(w, s_1, s_2, z_1) \\ &\leq \tilde{H}(s, w) + G_m z_1 \\ z_1 > 0 &: -\tilde{H}(s, w) + G_m z_1 \leq f(w, s_1, s_2, z_1) \\ &\leq \tilde{H}(s, w) + G_M z_1 \end{aligned} \tag{23}$$

$$\tilde{H}(s, w) = H_0 + H_1\|s\| + H_2\|w\|. \tag{24}$$

[1]The successive total time derivatives of s_1 must be evaluated along the trajectories of system (9)–(11) in the usual way.

[2]In this case, the $(\mathrm{m}+2)$th-order sliding dynamics does not depend on the control, i.e., it does not depend on the definition of solutions in $(\mathrm{m}+2)$th-order sliding mode.

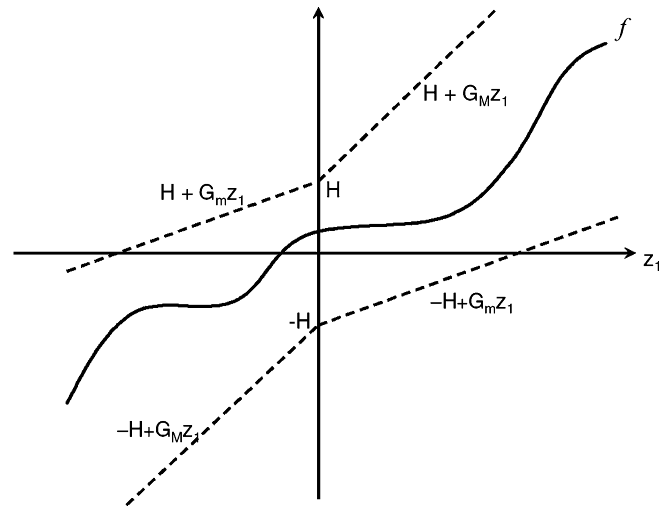

Fig. 1. Bounding curves for the function f.

Assumption 3: Consider the actuator dynamics (11) with the constant input $u(t) = \bar{U}, t \geq t_0$. Then, $\forall \varepsilon \in (0,1)$, there is $\gamma \in [\gamma_m, \gamma_M]$ and $N(\varepsilon) > 0$ such that

$$|z_1 - \gamma \bar{U}| \leq \varepsilon \gamma \bar{U} \qquad \forall t \geq t_0 + N(\varepsilon)\mu. \tag{25}$$

Assumption 1 prescribes a linear growth of $\|w(t)\|$ and $\|z(t)\|$ with respect to $\|s(t)\|$ and $|u|$, respectively. Assumption 2 guarantees that the virtual plant control input z_1, with large enough magnitude, can set the sign of f (see Fig. 1). The knowledge of constants $\xi_1, \xi_2, H_0, \ldots, G_M$ is mainly a technical requirement. With sufficiently large U, and $\beta \in [0.5, 1)$ sufficiently close to 1, stability can be insured regardless of $\xi_1, \ldots, G_M$. Assumption 3 requires a "nonintegrating" stable actuator dynamics whose settling time in the step response is $O(\mu)$. Note that γ and N are considered uncertain. Assumption 3 is always satisfied, e.g., in the special case of a linear asymptotically stable actuator dynamics.

Assume, only temporarily, that there exists a certain constant H such that $|\tilde{H}(s,w)| \leq H$, then conditions (23)–(24) reduce to the following:

$$\begin{aligned} z_1 \leq 0 &\Rightarrow -H + G_M z_1 \leq f(w, s_1, s_2, z_1) \leq H + G_m z_1 \\ z_1 > 0 &\Rightarrow -H + G_m z_1 \leq f(w, s_1, s_2, z_1) \leq H + G_M z_1 \end{aligned} \tag{26}$$

which can be represented graphically as in Fig. 1. The dashed lines limit the "admissible region" for the uncertain function f.

Consider the following tuning rules:

$$U = \frac{\eta H}{(1-\varepsilon)\gamma_m G_m} \quad \beta \in \left(1 - \frac{q(\eta - 1)}{\eta + 1 + \Delta}, 1\right) \tag{27}$$

$$\Delta = \frac{\gamma_M G_M (1+\varepsilon)}{\gamma_m G_m (1-\varepsilon)}, \qquad \eta > 1; \qquad \varepsilon \in (0,1); \qquad q \in (0,1). \tag{28}$$

In Theorem 1, we will show that with sufficiently large H and sufficiently small μ, control (12) and (27)–(28) *ensures* that condition $|\tilde{H}(\cdot)| \leq H$ holds, and furthermore, it is shown that a positively invariant μ-neighborhood of the second-order sliding set $s_1 = s_2 = 0$, defined as

$$O_\mu \equiv \{(s_1, s_2) : |s_1| \leq \rho_1 \mu^2, |s_2| \leq \rho_2 \mu\} \tag{29}$$

attracts in finite time the system trajectories.

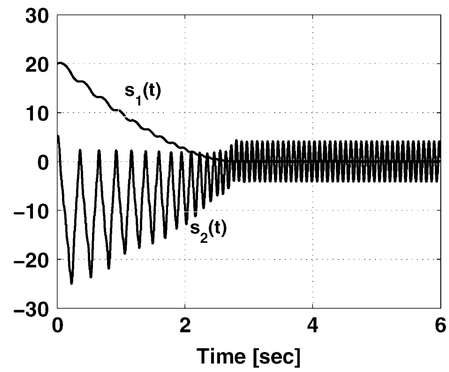

Fig. 2. Steady-state evolution of s_1 and s_2.

Theorem 1: Consider system (9)–(11), satisfying Assumptions 1–3 and driven by the G-SO controller (12) and (27)–(28). Then, if H is sufficiently large and μ is sufficiently small, the closed-loop system trajectories enter in finite time the invariant domain O_μ defined by (29), where ρ_1 and ρ_2 are proper constants.

Proof: See Appendix I.

Simulation Example: Consider system

$$\begin{aligned} \dot{w} &= -\sin(w) + s_1 + s_2 \\ \dot{s}_1 &= s_2, \dot{s}_2 = \frac{s_2}{1+s_2^2} + s_1 + w + [2 + \cos(z_1 + s_2)]z_1 \\ \mu \dot{z}_1 &= z_2 \quad \mu \dot{z}_2 = -z_1 - z_2 + u. \end{aligned} \tag{30}$$

The initial conditions and the controller parameters are $s_1(0) = 20, s_2(0) = 5, w(0) = 5, z_1(0) = z_2(0) = 0, U = 80$, and $\beta = 0.8$. Fig. 2 shows the time evolution of s_1 and s_2 when $\mu = 0.001$. The amplitude of chattering was evaluated as the maximum of $|s_1|$ and $|s_2|$ in the steady state, yielding $|s_1| \leq 0.0007$ and $|s_2| \leq 0.4$. We performed a second test using $\mu = 0.01$. The accuracy of s_1 changed to 0.07, and the accuracy of s_2 changed to 4, in perfect accordance with (29). Simulations show high-frequency *periodic* motions for s_1, s_2, and w. In the following, those "chattering" trajectories are investigated in further detail.

IV. Poincaré Map Analysis

We are going to derive conditions for the existence of stable periodic motions, in the vicinity O_μ of the second-order sliding set, in terms of the properties of some associated Poincaré maps. We will also give a constructive procedure to compute the parameters of chattering. Introducing the new variables $y_1 = \mu^{-2} s_1$ and $y_2 = \mu^{-1} s_2$, we can rewrite system (9)–(11) in the form

$$\dot{w} = g(w, \mu^2 y_1, \mu y_2) \tag{31}$$

$$\mu \dot{y}_1 = y_2 \quad \mu \dot{y}_2 = f(w, \mu^2 y_1, \mu y_2, z_1) \tag{32}$$

$$\mu \dot{z} = h(z, u(\mu^2 y_1)). \tag{33}$$

Note that the G-SO algorithm (12) is endowed by the homogeneity property $u(\mu^2 y_1) = u(y_1)$. To study the fast oscillations of the system under investigation, consider the original system in the fast time (OSFT)

$$dw/d\tau = \mu g(w, \mu^2 y_1, \mu y_2) \tag{34}$$

$$dy_1/d\tau = y_2 \quad dy_2/d\tau = f(w, \mu^2 y_1, \mu y_2, z_1) \tag{35}$$

$$dz/d\tau = h(z, u(y_1)) \tag{36}$$

and the *fast subsystem* (FS) with the "frozen" slow dynamics ($w \in \bar{W}$ is considered as a fixed parameter)

$$d\bar{y}_1/d\tau = \bar{y}_2 \quad d\bar{y}_2/d\tau = f(w, 0, 0, \bar{z}_1) \tag{37}$$

$$d\bar{z}/d\tau = h(\bar{z}, u(\bar{y}_1)). \tag{38}$$

Consider the solution of system (37) and (38) with initial condition

$$\bar{y}_1^+(0, w) = \bar{y}_1^0 \quad \bar{y}_2^+(0, w) = 0$$
$$\bar{z}^+(0, w) = \bar{z}^0 \quad f\left(w, \bar{y}_1^0, 0, \bar{z}_1^0\right) < 0 \tag{39}$$

such that $f(w, \bar{y}_1^0, 0, \bar{z}_1^0) < 0$ for all $w \in \bar{W}$. Suppose that for all $w \in \bar{W}$ there exists the smallest positive root of equation $\tau = T(w)$ for which $\bar{y}_2^+(T(w), w) = 0, f(w, \bar{y}_1^+(T(w), w), 0, \bar{z}_1^+(T(w), w)) < 0$. Now, we can define for all $w \in \bar{W}$ the Poincaré map

$$\left(\bar{y}_1^0, \bar{z}^0\right) \to \Xi\left(w, \bar{y}_1^0, \bar{z}^0\right) = \begin{bmatrix} \bar{y}_1(T(w), w) \\ \bar{z}(T(w), w) \end{bmatrix} \tag{40}$$

of the domain $f(w, y_1, 0, z_1) < 0$ on the surface $y_2 = 0$ into itself, generated by system FS (37) and (38) (the details of this mapping are described in Appendix II).

A. Sufficient Conditions for the Periodic Solution Existence

Let us suppose that the FS (37) and (38) has a nondegenerated isolated periodic solution and the following conditions hold.

Condition 1: $\forall w \in \bar{W}$, the FS (37) and (38) has an isolated $T_0(w)$-periodic solution

$$(\bar{y}_{10}(\tau, w), \bar{y}_{20}(\tau, w), \bar{z}_0(\tau, w)). \tag{41}$$

Condition 2: $\forall w \in \bar{W}$, the Poincaré map $\Xi(w, \bar{y}_1^0, \bar{z}^0)$ has an isolated fixed point $(\bar{y}_1^*(w), z^*(w))$ corresponding to the periodic solution (41).

Condition 3: $\forall w \in \bar{W}$, the eigenvalues $\lambda_i(w) (i = 1, \ldots, m+1)$ of the matrix

$$\frac{\partial \Xi}{\partial(y_1, z)}(w, \bar{y}_1^*(w), \bar{z}^*(w)) \tag{42}$$

are such that $|\lambda_i(w)| \neq 1$.

Condition 4: The averaged system

$$\frac{dw}{dt} = p(w) = \frac{1}{T_0(w)} \int_0^{T_0(w)} g(w, \bar{y}_{10}(\tau, w), \bar{y}_{20}(\tau, w), \bar{z}_0(\tau, w))\, d\tau \tag{43}$$

has an isolated, nondegenerated, equilibrium point w_0, such that

$$p(w_0) = 0 \quad \det\left|\frac{dp}{dw}(w_0)\right| \neq 0. \tag{44}$$

Theorem 2 is true.

Theorem 2: Under conditions 1–4, system (31)–(33) has an isolated periodic solution near the cycle

$$(w_0, \bar{y}_{10}(t/\mu, w_0), \bar{y}_{20}(t/\mu, w_0), \bar{z}_0(t/\mu, w_0)) \tag{45}$$

with period $\mu(T_0(w_0) + O(\mu))$.

Proof: See Appendix III.

B. Sufficient Conditions of Stability of Periodic Solution

Let $\nu_j(w_0) (j = 1, \ldots, n-2)$ be the eigenvalues of the matrix $(dp/dw)(w_0)$. Suppose that the periodic solution of FS (37) and (38) is exponentially orbitally stable and the equilibrium point of the averaged equations is exponentially stable.

Condition 5: $|\lambda_i(w)| < 1, (i = 1, \ldots, m+1)$.

Condition 6: $\nu_j(w_0)$ are real negative, i.e.,

$$\nu_j(w_0) < 0 \qquad \forall j = 1, \ldots, n-2.$$

Theorem 3: Under conditions 1–6, the periodic solution (45) of the system (31)–(33) is orbitally asymptotically stable.

Proof: See Appendix IV.

C. Example of Poincaré Map Analysis

Consider the following linear dynamics:

$$\begin{aligned} \dot{w} &= -w + y_1 \\ \dot{y}_1 &= y_2 \quad \dot{y}_2 = z \\ \mu\dot{z} &= -z + u \quad u = -\mathrm{sign}\left(y_1 - \frac{1}{2}y_{1M}\right). \end{aligned} \tag{46}$$

We have shown that analysis of periodic solutions can be performed by referring to the decomposition into fast and slow subsystem dynamics. The FS dynamics

$$dy_1/d\tau = y_2 \quad dy_2/d\tau = z \quad dz/d\tau = -z + u \tag{47}$$

generates the following Poincaré map $\Xi^+(y_1, z) = (\Xi_1^+(y_1, z), \Xi_2^+(y_1, z))$ of the domain $z < 0$ on the surface $y_2 = 0$ into the domain $z > 0$ of the same surface (see Appendix V for the detailed derivation)

$$\begin{aligned} \Xi_1^+(y_1, z) &= \frac{1}{2}y_1 + [(z+1)(1 - e^{-T_{sw}^+}) - T_{sw}^+]T_p^+ \\ &\quad + [(z+1)e^{-T_{sw}^+} - 2](T_p^+ + e^{-T_p^+} - 1) + \frac{1}{2}{T_p^+}^2 \\ \Xi_2^+(y_1, z) &= 1 + ((z+1)e^{-T_{sw}^+} - 2)e^{-T_p^+} \end{aligned} \tag{48}$$

where $T_{sw}^+ = T_{sw}^+(y_1, z)$ and $T_p^+ = T_p^+(y_1, z)$ are the smallest positive roots of the following:

$$\frac{1}{2}y_1 + (z+1)(e^{-T_{sw}^+} + T_{sw}^+ - 1) - \frac{1}{2}{T_{sw}^+}^2 = 0 \tag{49}$$

$$(z+1)(1 - e^{-T_{sw}^+}) + ((z+1)e^{-T_{sw}^+} - 2)(1 - e^{-T_p^+}) + T_p^+ - T_{sw}^+ = 0. \tag{50}$$

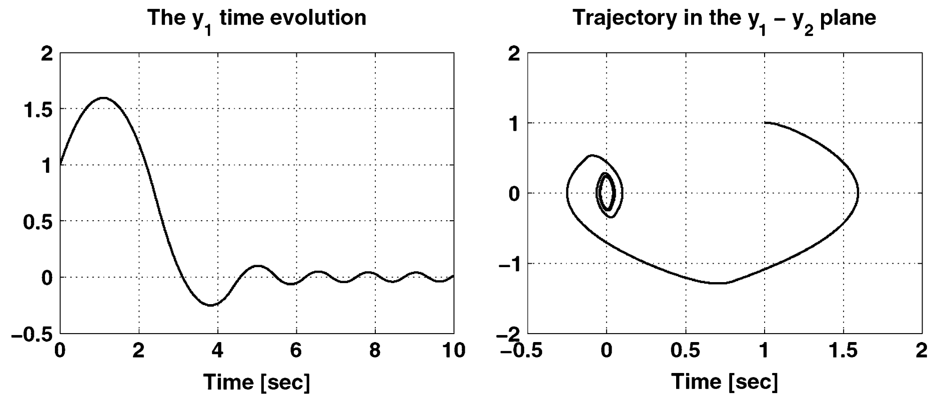

(a) (b)

Fig. 3. Transient trajectories with $\mu = 0.1$: (a) y_1 time evolution and (b) y_1-y_2 trajectory.

Taking into account the symmetry of dynamics (47) with respect to origin $(0, 0, 0)$, we can skip the computation of the map $\Xi^-(y_1, z)$ and rewrite condition for the periodicity of system (47) trajectory in the form

$$\Xi_1^+\left(y_{1p}^0, z_p^0\right) = -y_{1p}^0 \quad \Xi_2^+\left(y_{1p}^0, z_p^0\right) = -z_p^0. \tag{51}$$

The fixed points are

$$y_{1p}^0 \approx 3.95 \quad z_p^0 \approx -0.96 \tag{52}$$

and the switching times are

$$\bar{T}_{sw}^+ \approx 2.01 \quad \bar{T}_p^+ \approx 3.93 \quad \bar{T}_0^+ = \bar{T}_{sw}^+ + \bar{T}_p^+ \approx 5.94. \tag{53}$$

The Frechet derivatives entering the Jacobian matrix are given by

$$\begin{aligned}\mathbf{J} = \frac{\partial \Xi}{\partial(\mathbf{y_1}, \mathbf{z})} &= \begin{bmatrix} \left.\dfrac{\partial \Xi_1}{\partial y_1}\right|_{(y_{1p}^0, z_p^0)} & \left.\dfrac{\partial \Xi_1}{\partial z}\right|_{(y_{1p}^0, z_p^0)} \\ \left.\dfrac{\partial \Xi_2}{\partial y_1}\right|_{(y_{1p}^0, z_p^0)} & \left.\dfrac{\partial \Xi_2}{\partial z}\right|_{(y_{1p}^0, z_p^0)} \end{bmatrix} \\ &= \begin{bmatrix} -0.4894 & 1.5273 \\ 0.0095 & -0.0147 \end{bmatrix}. \end{aligned} \tag{54}$$

The eigenvalues of matrix $\mathbf{J}$ are $\mathrm{eig}(\mathbf{J}) = [-0.5182, 0.0141]$, i.e., they are both lying within the unit circle of the complex plane, which implies that the periodic solution of the FS (47) is orbitally asymptotically stable.

The averaged equations for the internal dynamics has the form $\dot{w} = -w$. Now, from Theorems 1–3, it follows that 1) system (46) has an orbitally asymptotically stable periodic solution lying in the O_μ boundary layer (29) of the second-order sliding set $y_1 = y_2 = 0$ and 2) in the steady state, the internal dynamics w variable features a $O(\mu)$ deviation from the equilibrium point $w = 0$ of the averaged solution. It is also expected from Theorem 2 that the period of oscillation is $O(\mu)$.

The period and amplitude of the periodic solutions of (46) can be easily inferred from (52) and (53) via proper μ-dependent scaling.

D. Simulations

These results have been checked by means of computer simulations. The initial conditions are $w(0) = y_1(0) = y_2(0) = z(0) = 1$. The value $\mu = 0.1$ was used in the first test. It is expected, on the basis of the previous considerations, that y_1 exhibits a steady oscillation with amplitude $\mu^2 y_{1p}^0 \approx 0.0395$ and period $2\mu T_p^+ \approx 1.18s$. The plots in Fig. 3 highlight the convergence to the periodic solution starting from initial conditions outside from the attracting O_μ domain.

Now, let us check the period and the amplitudes of the steady solutions of y_1, y_2, and w. The corresponding plots are reported in Fig. 4. The y_1 time evolution features the expected amplitude and period previously computed. System (46) was also simulated with a different value of μ, say $\mu = 0.01$. We expect that the period of the oscillation scales down by factor 10, becoming near $0.12s$. We also expect that the amplitude of the oscillation of y_1 and y_2 scales down by factors 100 and 10, respectively, and that w is closer to the equilibrium point $w = 0$ of the averaged solution. This is confirmed by the plots in Fig. 5.

V. Frequency-Domain Analysis

The Poincaré-map-based analysis provides an exact but complicated approach. Therefore, the use and adaptation of frequency methods for the chattering analysis in control systems with the fast actuators driven by 2-SMC G-SO algorithms seems expedient. However, this approach applies to linear dynamics. For this reason, in this section, we assume that the plant plus actuator dynamics are either linear or linearized in the conventional sense in a small vicinity of the domain (29).

Section V-A discusses the problem of local linearization and Section V-B states formally the analysis problem. Section V-C is devoted to the describing function approach (see, for example, [2]) to the analysis of the G-SO algorithm in the closed loop. This approach is approximate and requires the linearized system (actuator and plant) being a low-pass filter. This assumption is equivalent to the hypothesis of the actuator being fast. Thus, Section V-D presents the modified Tsypkin locus [43] method, which does not require the filtering hypothesis, and, furthermore:

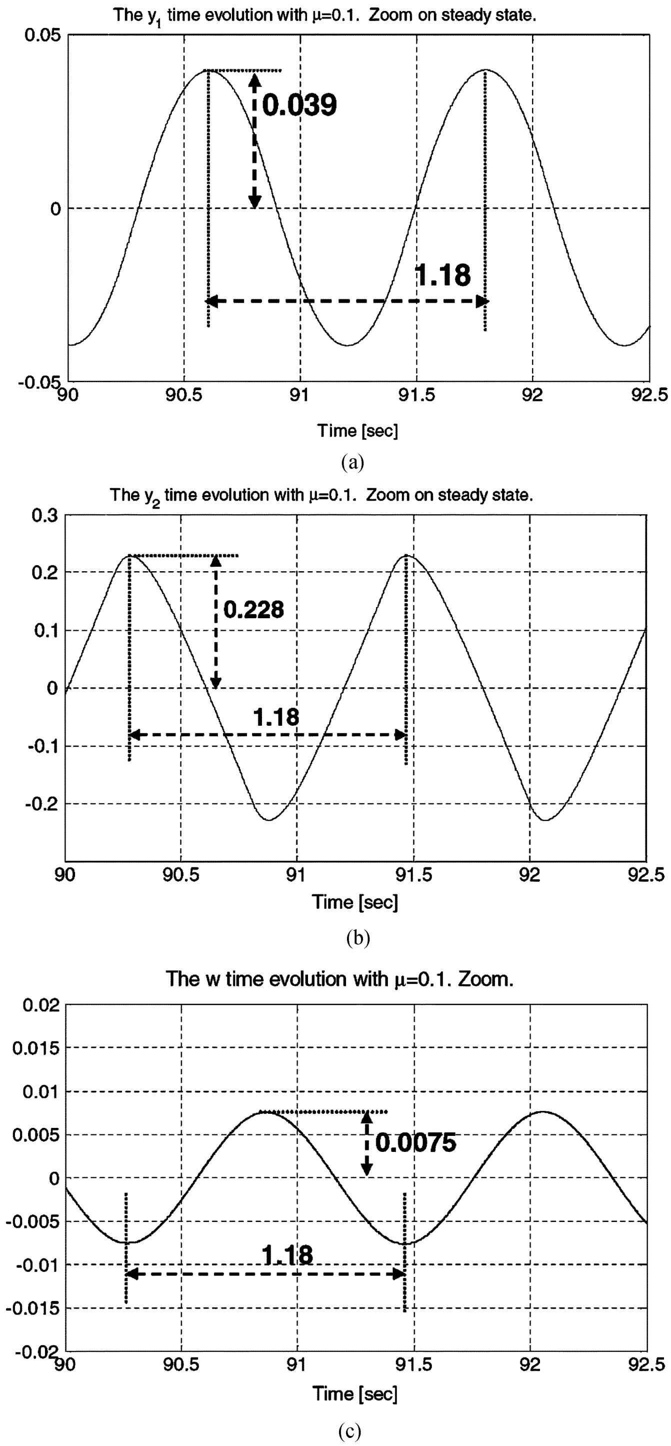

Fig. 4. Steady-state analysis with $\mu = 0.1$: (a) y_1 time evolution, (b) y_2 time evolution, and (c) w time evolution.

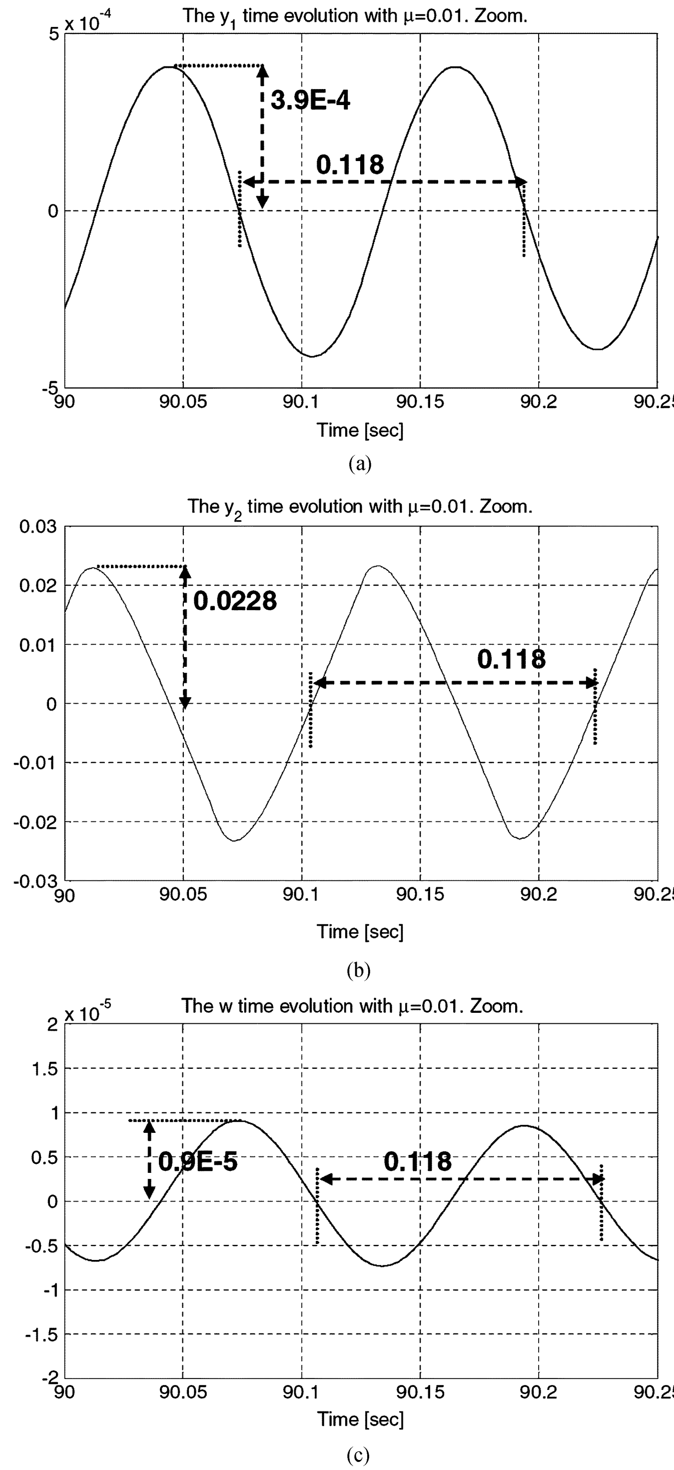

Fig. 5. System (46) with $\mu = 0.01$: (a) y_1 time evolution, (b) y_2 time evolution, and (c) w time evolution.

— provides exact values of the frequency and the amplitude of the periodic motion as a solution of an algebraic equation and the use of an explicit formula, respectively;

— does not require for actuator to be fast.

A. Local Linearization of System (9)–(11)

We have shown that controller (12) can provide for the appearance of a stable sliding mode of order $m + 2$, and that the system (9)–(12), with full state vector $\xi = [w^T, s^T, z^T]$, has a fixed equilibrium point $\xi_0 = (w_0, 0, z_0)$ (see Remark 4). The constant equilibrium value for the actuator input is $u = u_0(w_0, z_0)$, then it is reasonable to linearize the system (9)–(12) in the small neighborhood of the point ξ_0 by considering the constant control value u_0 in the terms depending on it.

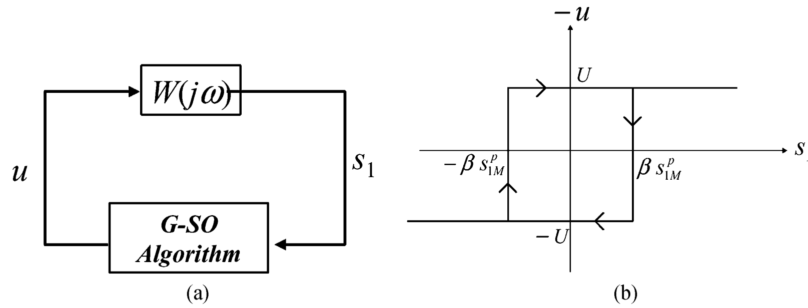

Fig. 6. (a) Closed-loop system with the G-SO algorithm. (b) Control characteristic in steady state.

Simple computations yield the following linearized dynamics:

$$\dot{\xi} = \mathbf{A}\xi + \mathbf{B}u$$
$$s_1 = \mathbf{C}\xi \tag{55}$$
$$\mathbf{A} = \begin{bmatrix} \frac{\partial g}{\partial s_1} & \frac{\partial g}{\partial s_2} & \frac{\partial g}{\partial w} & 0 \\ 0 & 1 & 0 & 0 \\ \frac{\partial f}{\partial s_1} & \frac{\partial f}{\partial s_2} & \frac{\partial f}{\partial w} & \frac{\partial f}{\partial z} \\ 0 & 0 & 0 & \frac{\partial h}{\partial z} \end{bmatrix} \tag{56}$$
$$\mathbf{B} = \left[0, 0, \ldots, 0, \frac{\partial h}{\partial u}\right]^T \qquad \mathbf{C} = [0, \ldots, 0, 1, 0, \ldots, 0] \tag{57}$$

where the nonzero element of $\mathbf{C}$ is represented by its $(n-1)$th entry according to the state-output relationship $s_1 = \mathbf{C}\xi$. The characteristic matrix $\mathbf{A}$ and control gain vector $\mathbf{B}$ contain some partial derivatives of functions f, g, and h which must be evaluated in the considered equilibrium point ξ_0 and equilibrium control value u_0.

Because the system trajectories will converge to an $O(\mu)$ vicinity of the equilibrium, the accuracy of the linear approximation depends on the μ parameter; the smaller μ is, the higher the accuracy becomes. The transfer function and harmonic response of the linearized system (55)–(57), which is asymptotically stable by construction, can be computed straightforwardly.

B. Problem Statement

Consider the transfer function $W(s)$ of a linear stable dynamics and the associated harmonic response $W(j\omega)$. The closed-loop system with the G-SO algorithm is presented in Fig. 6(a).

The term s_{1Mi} appearing in the switching function of control (12) changes stepwise at the time instants $t_{Mi}(\mathrm{i} = 1, 2, \ldots)$ at which $\dot{s}_1(t_{Mi}) = 0$. During the periodic motion, s_{1Mi} is an alternating (ringing) series of positive and negative values, i.e., $s_{1M}^p, -s_{1M}^p, s_{1M}^p$, and $-\ s_{1M}^p$ (here, "p" stands for periodic). The control sign change would occur at the time when the plant output is equal to $\pm\beta s_{1M}^p$. Therefore, in the periodic motion, the control function (12) can be represented by the hysteretic relay nonlinearity in Fig. 6(b). This representation opens the way for the use of the frequency-domain methods developed for analysis of relay feedback systems [2], [43]. The main difference from the conventional application of the existing methods is that the hysteresis value is unknown *a priori*.

C. DF Analysis

DF analysis is a simple approach which can provide in most cases a sufficiently accurate estimate of the frequency and the amplitude of a possible periodic motion. The main difference between the considered case and a conventional relay system is that the hysteresis value βs_{1M}^p is actually *unknown*. To solve this problem, we can consider that during a periodic motion the extreme values of the output coincide, in magnitude, with its amplitude. Therefore, s_{1M}^p is actually the unknown amplitude of the periodic motion. The DF of the relay with a negative hysteresis is given as follows [2]:

$$q(A_y) = \frac{4c}{\pi A_y}\sqrt{1 - \frac{b^2}{A_y^2}} + j\frac{4bc}{\pi A_y^2} \tag{58}$$

where $b = \beta y_M^p$ is a half of the hysteresis, $c = U$ is the relay amplitude, and $A_y = y_M^p$ is the amplitude of the harmonic input to the relay. Then, we can exploit the given relationships between the hysteresis parameters and the oscillation parameters in order to obtain the following expression for the DF of the G-SO algorithm:

$$q(A_y) = \frac{4U}{\pi A_y}\left(\sqrt{1-\beta^2} + j\beta\right). \tag{59}$$

A periodic solution can be found from the harmonic balance equation $W(j\omega) = -(1/q(A_y))$ [2], where the negative reciprocal of the DF (59) is as follows:

$$-\frac{1}{q} = -\frac{\pi A_y}{4U}(\sqrt{1-\beta^2} - j\beta). \tag{60}$$

As usual, the periodic solutions correspond to the points of intersection of the $W(j\omega)$ and $-1/q(A_y)$ loci, the latter being a straight line backing out of the origin with a slope that depends only on parameter β, as depicted in Fig. 7.

Therefore, a periodic motion may occur if at some frequency $\omega = \bar{\omega}$ the phase characteristic of the actuator-plant transfer function W is equal to $-180^0 - \arcsin(\beta)$. If such a requirement is fulfilled, so that intersection between the two plots occurs, then the frequency and the amplitude of the periodic solution can be derived from the "crossover" frequency $\bar{\omega}$ and from the magnitude of vector $\overline{OA}$ in Fig. 7, respectively. An intersection point will certainly exist if the overall relative degree of the combined actuator-plant degree is three or higher.

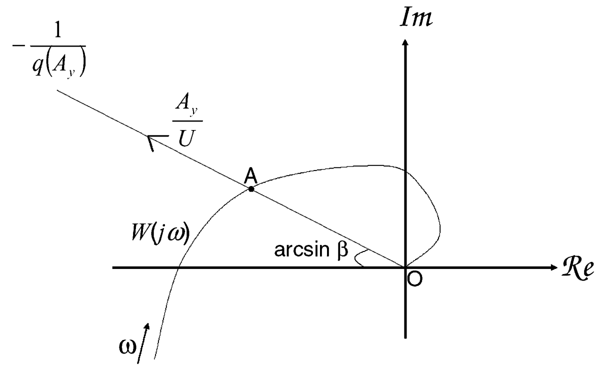

Fig. 7. DF analysis.

TABLE I
PERIODIC MOTION ANALYSIS OF SECTION VI-A

	Frequency [rad sec^{-1}]	Amplitude
DF	24.9	0.0020
Modified Tsypkin Locus	23.26	0.0024
Simulation	22.25	0.0025

D. Exact Frequency-Domain Analysis via Modified Tsypkin Locus

The DF analysis given previously provides a simple and systematic, but approximate, evaluation of the magnitude and frequency of the periodic motions in linear systems driven by the G-SO algorithm (12). An exact solution, **which does not require the actuator to be fast**, can be obtained via application of the Tsypkin's method [43].

The Tsypkin locus approach involves computing the following complex function $\Lambda(\omega)$, called the Tsypkin locus:

$$\Lambda(\omega) = \frac{4c}{\pi}\sum_{k=1}^{\infty}\mathrm{Re}\{W[(2k-1)\omega]\} + j\frac{4c}{\pi}\sum_{k=1}^{\infty}\frac{1}{2k-1}\cdot\mathrm{Im}\{W[(2k-1)\omega]\} \quad (61)$$

where c is the magnitude of the relay output. The frequency $\bar{\omega}$ of the periodic solution can be found by solving the equation $\mathrm{Im}\Lambda(\bar{\omega}) = -b$, where $2b$ is the hysteresis value. Unfortunately, the hysteresis b is a function of the unknown amplitude of the oscillations, and the explicit formula for the "true" amplitude of the oscillations does not exist.

The problem of the exact frequency-domain analysis can be conveniently solved by the technique presented in the following. Introduce the complex function $\Phi(\omega)$ as follows:

$$\Phi(\omega) = -\sqrt{[A_y(\omega)]^2 - y^2\left(\frac{\pi}{\omega},\omega\right)} + jy\left(\frac{\pi}{\omega},\omega\right) \quad (62)$$

where $y((\pi/\omega),\omega)$ is the value of the system output at the time instant when the relay switches from $-V_M$ to V_M (π/ω is half a period in the periodic motion and $t=0$ is assumed, without loss of generality, to be the time of the relay switch from V_M to $-V_M$) and $A_y(\omega)$ is the amplitude of the plant output in the assumed periodic motion of frequency ω

$$A_y = \max_{t\in[0,T]}|y(t,\omega)|. \quad (63)$$

$y(t,\omega)$ can be computed by means of its Fourier series

$$\begin{aligned} y(t,\omega) &= \frac{4c}{\pi}\sum_{k=1}^{\infty}\frac{1}{k}\sin\left(\frac{1}{2}\pi k\right)\sin[k\omega t+\varphi(k\omega)]L(\omega k) \\ &= \frac{4c}{\pi}\sum_{k=1}^{\infty}\frac{(-1)^{k+1}}{2k-1}\sin[(2k-1)\omega t+\varphi((2k-1)\omega)] \\ &\quad \cdot L((2k-1)\omega) \end{aligned} \quad (64)$$

where $\varphi(k\omega) = \arg W(jk\omega)$ and $L(k\omega) = |W(jk\omega)|$ are the phase and magnitude of $W(j\omega)$ at the frequency $k\omega$, respectively.

The frequency-dependent variable $A_y(\omega)$ can be computed by using (63) and (64) and $y((\pi/\omega),\omega)$ as the imaginary part of (61) or via using the Fourier series (64). As a result, function $\Phi(\omega)$ has the same imaginary part as the Tsypkin locus, and the magnitude of function $\Phi(\omega)$ at the intersection point represents the amplitude of the periodic solution.

Having computed the function $\Phi(\omega)$, we can carry out the graphical analysis of possible periodic motions the same way as it was done previously via the DF technique, simply replacing the Nyquist plot of $W(j\omega)$ with the function $\Phi(\omega)$ given by (62). Let us call the function $\Phi(\omega)$, given by (62), the *modified Tsypkin locus.*

VI. EXAMPLES OF FREQUENCY-DOMAIN ANALYSIS

A. Linear Case

Consider $W(s)$ being the cascade connection of the second-order linear plant $W_p(s)$ and the first-order dynamic actuator $W_a(s)$

$$W_p(s) = \frac{1}{s^2+s+1} \quad W_{a1}(s) = \frac{1}{0.01s+1}. \quad (65)$$

The loop is closed via the G-SO algorithm (12) having the switching anticipation parameter $\beta = 0.2$ and control magnitude $U = 1$. The approximate and theoretically exact parameters of the periodic solution (obtained by means of the DF and modified Tsypkin locus techniques, respectively) were computed, and the "true" values were also found by computer simulation (see Table I). Higher accuracy of the modified Tsypkin method is apparent.

In Fig. 8(a), the graphical DF analysis is depicted. The magnitude of W at the intersection point is $M = |W(j24.8)| \approx 0.0016$, then the estimated oscillation amplitude is $\hat{A}_y = 4MU/\pi \approx 0.002$. Fig. 8(b) and (c) refers to the modified Tsypkin analysis. Fig. 8(b) shows the modified Tsypkin locus drawn in the frequency interval $\omega \in$ [1, 300] rad/s, while Fig. 8(c) focuses on the frequency range $\omega \in$[22, 24] rad/s where the intersection with the negative reciprocal DF is found. Fig. 9 provides the results of the computer simulation of this system.

The higher accuracy of the modified Tsypkin analysis, with respect to the DF analysis, is justified by the theoretical analysis presented previously. The mismatch of the simulation values with respect to those values computed via the modified Tsypkin locus (which are theoretically exact) is caused by factors of numerical approximation such as truncation of the series (64),

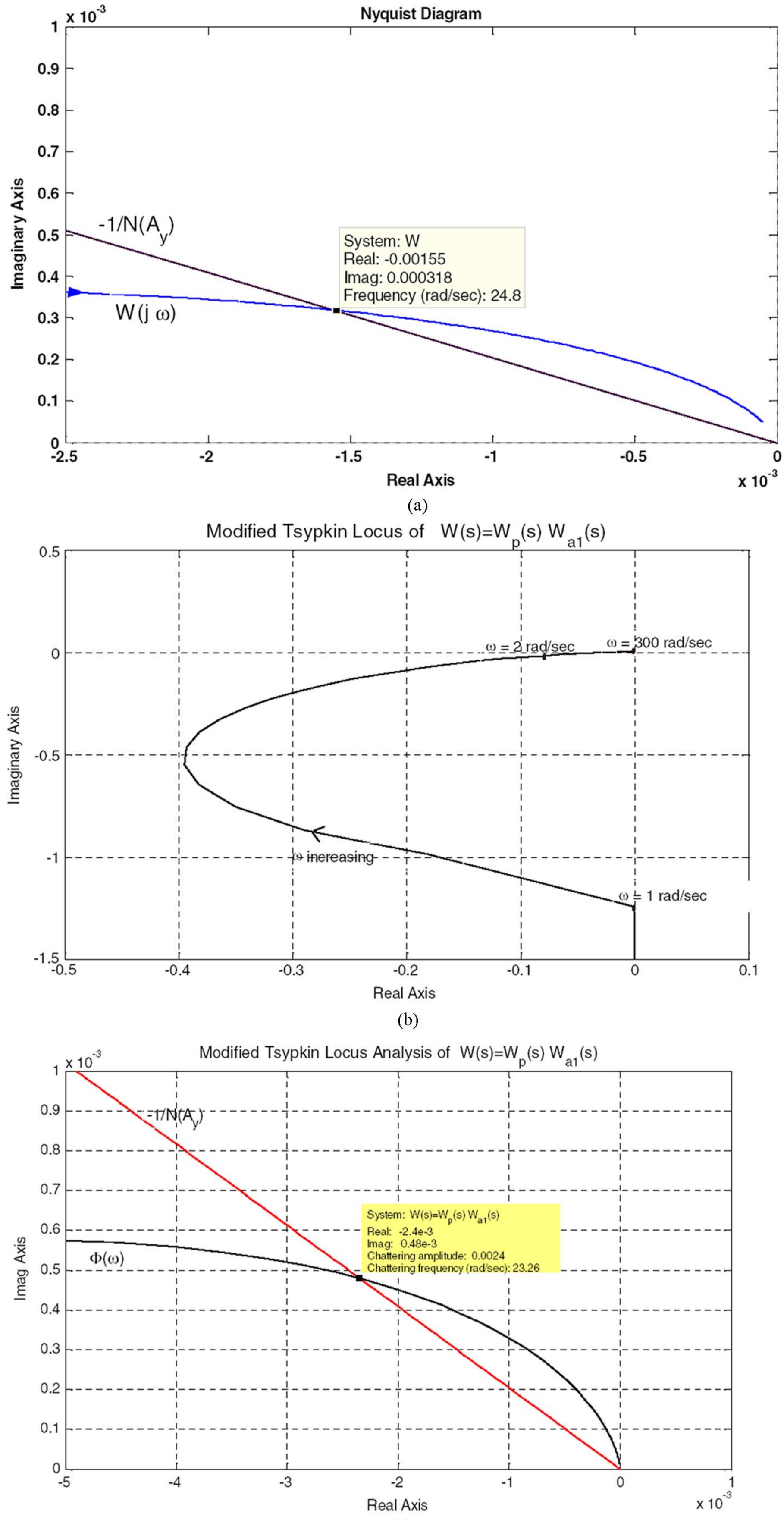

Fig. 8. Section 6–A. (a) DF Analysis. (b) and (c) Modified Tsypkin analysis.

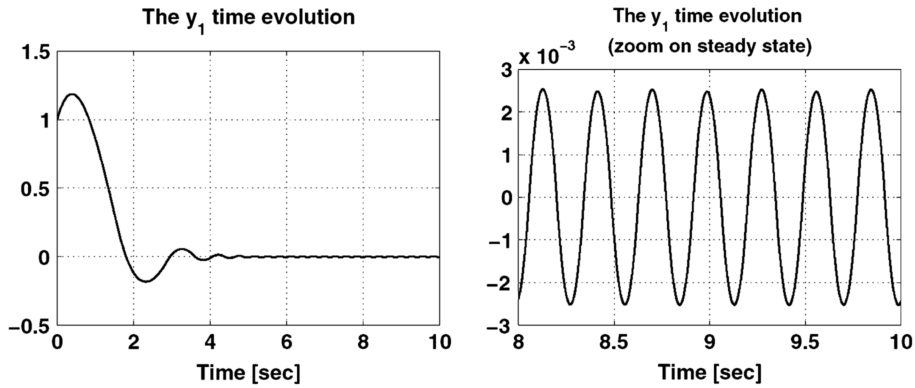

Fig. 9. Section 6–A. The periodic solution.

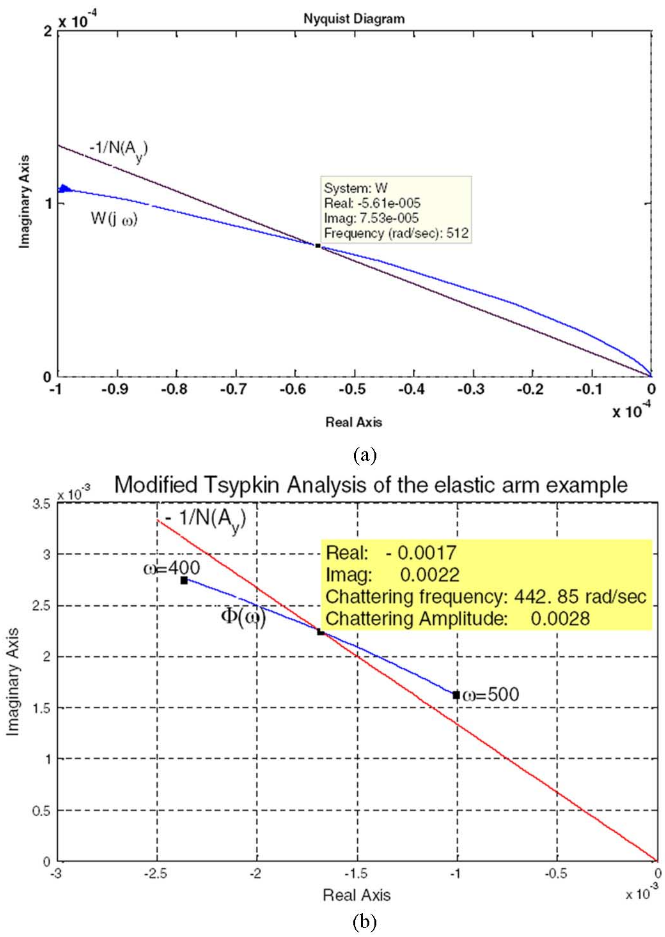

Fig. 10. Elastic arm example. (a) DF analysis. (b) Modified Tsypkin analysis.

roundoffs, and discrete-time integration of the simulation example.

B. Linearization-Based Analysis

Consider the simplified model of the rotating arm driven by a torque motor through an elastic friction link

$$\frac{1}{2}ML^2\ddot{q}_1 + B_1\dot{q}_1 + \frac{1}{2}MgL\sin(q_1) = K(q_2 - q_1) + B(\dot{q}_2 - \dot{q}_1)$$
$$J\ddot{q}_2 + B_2\dot{q}_2 + K(q_2 - q_1) + B(\dot{q}_2 - \dot{q}_1) = \tau \qquad (66)$$

where q_1 and q_2 represent the arm and motor coordinates, respectively, M and L are the mass and length of the arm, B_1 is the arm friction term, K is the joint stiffness coefficient, B is the link viscous friction coefficient, J and B_2 are the motor inertia and viscous friction coefficient measured at the link-side of the gears, and τ is the electromagnetic torque exerted by the motor. The electrical dynamics of the torque servo drive is accounted for by adding a first-order filter between the "command" torque τ^* (reference input to the torque-controlled servo drive) and the actual torque profile τ, according to the following:

$$\tau = \frac{1}{1+\mu s}\tau^* \quad \mu = 0.01. \qquad (67)$$

Let only the link coordinates be available for measurement and define the sliding variable as $s_1 = \dot{q}_2 + c(q_2 - q_1^*)$, with $c > 0$ and q_1^* being a set-point value. The dynamics (66) restricted onto the manifold $s_1 = 0$ is now briefly discussed. If s_1 tends to zero, then $q_2 \to q_1^*$ and $\dot{q}_2 \to 0$ exponentially. Considering these two conditions into the first (66) yields an exponentially stable error variable $q_1 - q_1^*$, as it can be proven by standard Lyapunov analysis.

In order to obtain a continuous torque profile, we add an integrator at the input side [7]. The time derivative of the command torque is set via the G-SO controller with $\beta = 0.8$ and $U = 20$. The following parameters were used: $M = 1$ kg, $L = 1$ m, $J = 0.01$ kgm^2, $B_1 = 0.1$ Nms, $B_2 = 1$ Nms, $K = 100$ Nm, $B = 1$ Nms, $q_1^* = \pi/3$, and $c = 3$. The linearized dynamics can be expressed in terms of the deviation variables $\bar{\delta}q = [\delta q_1, \delta q_2, \delta\dot{q}_1, \delta\dot{q}_2]$ and $\delta s_1 = s_1$ as (68) and (69), shown at the bottom of the next page.

The linearized plant can, therefore, be presented as in Fig. 6(a) with

$$W(j\omega) = \frac{\mathbf{C}(j\omega\mathbf{I} - \mathbf{A})^{-1}\mathbf{B}}{j\omega(j\omega\mu + 1)}. \qquad (70)$$

As shown in Fig. 10(a), DF analysis yields the following value of the chattering frequency $\hat{\omega} = 512$ rad/s. The magnitude of W in the intersection point is $M = |W(j512)| \approx 9.4e-5$, and the oscillation amplitude is $\hat{A}_y = 4MU/\pi \approx 0.0024$. Analysis via the modified Tsypkin locus [see Fig. 10(b)] gives the following frequency and amplitude: $\hat{\omega} = 442.8$ rad/s and $\hat{A}_y = 0.0028$.

Simulations of the nonlinear model (66) and (67) with $\mu = 0.01$ provide the steady-mode time evolution of $s_1$depicted in

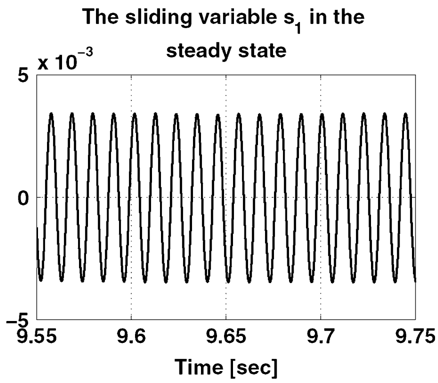

Fig. 11. The s_1 time evolution in the steady state.

TABLE II
PERIODIC MOTION ANALYSIS OF SECTION VI-B WITH $\mu = 0.001$

	Frequency [rad sec^{-1}]	Amplitude
Modified Tsypkin Locus	1.68E+3	4.99E-4
Simulation	1.61E+3	5E-4

Fig. 11. The observed amplitude and frequency of the oscillation are $A_y \approx 0.0029$ and $\bar{\omega} \approx 436$ rad^{-1}.

The periodic motion analysis and the tests were also repeated with a smaller value of $\mu = 0.001$. The contraction of the boundary layer O_μ was expected in accordance with (29), which is confirmed as the reduction of the amplitude of chattering presented in Table II. The frequency of chattering increases, which agrees with the fact that the control system bandwidth becomes larger.

VII. CONCLUSION

A systematic approach to analysis of chattering in control systems with fast actuators driven by the second-order sliding-mode G-SO controller is proposed. Analysis is carried out in the state space and frequency domains for linear and nonlinear plants. It is shown that the system motions always converge to the O_μ domain (29) of approximation with respect to the fast actuator's time constant μ, and, under some conditions, they converge to a limit cycle fully contained in this domain. The main results of this paper are as follows.

For nonlinear plants and nonlinear actuators, the results are as follows.

- The amplitude of chattering in a small vicinity of the sliding surface and its derivative are estimated.
- Sufficient conditions for the orbital asymptotic stability of the fast periodic motions are obtained in terms of the properties of corresponding Poincaré maps.

For linear plants and linear actuators, the results are as follows.

- The describing function and the Tsypkin locus are adapted to accommodate the task of analysis of the 2-SM system driven by the G-SO controller; the DF and the modified Tsypkin locus are obtained in the form of analytic expressions.
- A methodology of approximate analysis of the amplitude and the frequency of chattering via application of the DF method is proposed.
- A methodology of exact analysis of the amplitude and the frequency of chattering via application of the modified Tsypkin's method is given.

APPENDIX I
PROOF OF THEOREM 1

The Proof is divided in five steps.

Step A) There exists $t_{M_1} \geq t_0$ such that $s_2(t_{M_1}) = 0$.

Step B) There exists a sequence of time instants $t_{M_j}, j \geq 2$ such that $s_2(t_{M_j}) = 0$.

Step C) There is $\rho_1^* > 0$ such that, if $|s_{1M_j}| > \rho_1^* \mu^2$, then

$$|s_{1M_{j+h}}| \leq \max\{\beta, q\} |s_{1M_j}|, \qquad 0 < q < 1; \qquad h \in \{1, 2\}. \tag{71}$$

Step D) There exists a positive constant H overestimating $|\tilde{H}(s, w)|$.

Step E) There are $\rho_1 > 0$ and $\rho_2 > 0$ such that the domain O_μ (29) is invariant.

Step A. Let $t_0 = 0$ be the initial time instant and assume, without loss of generality that $s_1(0) > 0$. If $s_1(0)s_2(0) \geq 0$, then for any $t \in [0, t_{M_1})$, $s_2(t)$ cannot be zero. Thus, $|s_1(t)|$ is

$$\begin{aligned}
\dot{\bar{\delta}}q &= \mathbf{A}\bar{\delta}q + \mathbf{B}\tau \\
\delta s_1 &= \mathbf{C}\bar{\delta}q
\end{aligned} \tag{68}$$

$$\mathbf{A} = \begin{bmatrix} 0 & 0 & 1 & 0 \\ 0 & 0 & 0 & 1 \\ -\left[\dfrac{g}{L}\cos(q_1^*) + \dfrac{2K}{ML^2}\right] & \dfrac{2K}{ML^2} & -\dfrac{2(B_1+B)}{ML^2} & \dfrac{2B}{ML^2} \\ \dfrac{K}{J} & -\dfrac{K}{J} & \dfrac{B}{J} & -\dfrac{B+B_2}{J} \end{bmatrix}$$

$$\mathbf{B} = \begin{bmatrix} 0 \\ 0 \\ 0 \\ \dfrac{1}{J} \end{bmatrix} \quad \mathbf{C}^T = \begin{bmatrix} 0 \\ c \\ 0 \\ 1 \end{bmatrix}. \tag{69}$$

increasing and $u(t) = -U$ for any $t \in [t_0, t_{M_1})$. By Assumption 3 and (27) and (28)

$$z_1 \leq -(1-\varepsilon)\gamma U \leq -\frac{\eta H}{G_m} \quad N\mu \leq t \leq t_{M_1}. \tag{72}$$

Hence, by (26), the "reaching condition" $\dot{s}_2(t)s_2(t) < -H[\eta+1]|s_2(t)|$ holds at $t \in [N\mu, t_{M_1})$, which proves the claim. If $s_1(0)s_2(0) < 0$, by construction, $|s_1(t)|$ is decreasing when $t \in [0, t_{M1}]$. This means that there exists $t_c \in (t_0, t_{M_1})$ at which $s(t_c) = \beta s_1(0)$. Therefore, control u is such that $u = U$ for $t \in [t_c, t_{M_1})$. By taking into account Assumption 3 and (27) and (28), the same reaching condition holds over the time interval $t \in [t_c + N\mu, t_{M_1}]$, which proves the claim.

Step B. It is easy to show that, because of the actuator dynamics, if $\dot{s}_2(t_{M_1})s_1(t_{M_1}) > 0$, then $\dot{s}_2(t_{M_2})s_1(t_{M_2}) < 0$. It can be, therefore, assumed that at $t = t_{M1}$ condition $\dot{s}_2(t_{M_1})s_1(t_{M_1}) < 0$ holds, which implies that at $t \geq t_{M_1}^+$ the system trajectory enters one of the even quarters $s_1 s_2 < 0$. Let us assume, without loss of generality, that $s_1(t_{M_1}) > 0$ and refer to the plot in Fig. 12. All possible actual trajectories of the uncertain system are confined between the limit curves $a, \ldots, d$ in Fig. 12. Such curves are computed by a worst-case analysis which considers the limit values of the uncertainty f as specified in (26).

There is t_{c_1} such that $s_1(t_{c_1}) = \beta s_{1M_1}$, then control u is given as follows:

$$u(t) = \begin{cases} -U, & t_{M_1} \leq t < t_{c_1} \\ U, & t_{c_1} \leq t < t_{M_2} \end{cases}. \tag{73}$$

By Assumption 3 and (26)–(28), there exists $t_{M_2} > t_{M_1}$ such that $s_2(t_{M_2}) = 0$. By iteration, the claim is proven.

Step C. We are going to prove that there exist $\rho_1^* > 0$ and $q \in (0,1)$ such that, as long as $|s_{1Mi}| > \rho_1^* \mu^2$, then

$$s_{1M,i}s_{1M,i+1} < 0 \Rightarrow \begin{cases} |s_{1M,i+1}| \leq q|s_{1Mi}| \\ s_{1M,i+1}\ddot{s}_{1M,i+1} < 0 \end{cases} \tag{74}$$

$$s_{1M,i}s_{1M,i+1} > 0 \Rightarrow \begin{cases} |s_{1M,i+1}| < |s_{1M,i+2}| \leq q|s_{1M,i}| \\ s_{1M,i+2}\ddot{s}_{1M,i+2} < 0 \end{cases}. \tag{75}$$

The property is proven for $i=1$. Refer to the plot in Fig. 12. We aim at evaluating the points $\underline{s}_{1M_2}$ and $\bar{s}_{1M_2}$. By algebraic computations, it yields that singular point $P_{M2} \equiv (s_{1M_2}, 0)$, achieved at $t = t_{M2}$ when $s_2(t_{M2}) = 0$, is such that

$$\underline{s}_{1M2} \leq s_{1M2} \leq \bar{s}_{1M2} \tag{76}$$

$$\underline{s}_{1M2} = \beta s_{1M1} - \frac{(1-\beta)(H + G_M\gamma_M(1+\varepsilon)U)}{G_m\gamma_m(1-\varepsilon)U - H}s_{1M1} - \varphi_1\mu\sqrt{s_{1M1}} - \varphi_2\mu^2$$

$$\bar{s}_{1M2} = \beta s_{1M1} - \frac{(1-\beta)(G_m\gamma_m(1-\varepsilon)U - H)}{H + G_M\gamma_M(1+\varepsilon)U}s_{1M1} \tag{77}$$

with φ_1 and φ_2 being positive constants. The contraction condition (71), with $j = h = 1$, is then equivalent to

$$\underline{s}_{1M2} \geq -qs_{1M1}. \tag{78}$$

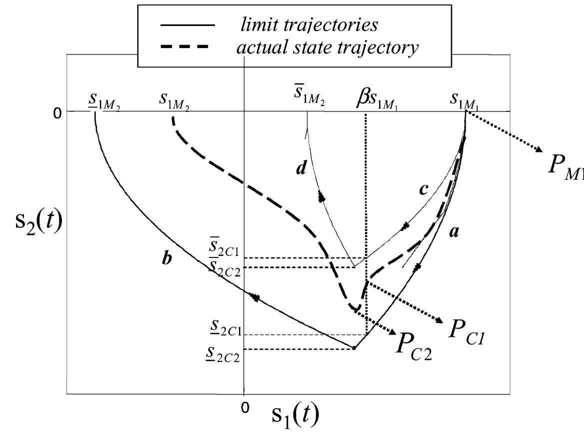

Fig. 12. Actual and limit trajectories in the s_1-s_2 plane.

Equation (78) can be rewritten as

$$\Omega_1 s_{1M1} + \varphi_1\mu\sqrt{s_{1M1}} + \varphi_2\mu^2 \leq (\beta + q)\, s_{1M1}$$

$$\Omega_1 = \frac{(1-\beta)[H + G_M\gamma_M(1+\varepsilon)U_M]}{G_m(1-\varepsilon)U - H}. \tag{79}$$

To solve (79), let us introduce the new variable $\rho_1 = (s_{1M1}/\mu^2)$ and rewrite (79) as

$$\Omega_1\rho_1 + \varphi_4\sqrt{\rho_1} + \varphi_3 \leq (\beta+q)\rho_1. \tag{80}$$

If condition $\Omega_1 < \beta + q$ holds, then the slope of the right-hand side of (80) is less than $\beta + q$ and a nonempty solution interval of (80) exists. Manipulating condition $\Omega_1 < \beta + q$, one obtains directly the second of (27). The resulting solution interval of (80) is $\rho_1 \geq \underline{\rho}_1$ where $\underline{\rho}_1$ is the unique positive root of equation $\Omega_1\rho_0 + \varphi_4\sqrt{\rho_0} + \varphi_3 = (\beta+q)\rho_0$. Then, by considering (76) and (77), there is $\rho_1^* > \underline{\rho}_1$ such that, as long as

$$|s_{1M1}| \geq \rho_1^*\mu^2 \tag{81}$$

then $|s_{M3}|$ is contractive with respect to $|s_{M1}|$ according to (75). Convergence takes place in finite time since there is $k > 0$ such that $t_{M,i+1} - t_{M,i} \leq k\sqrt{|s_{Mi}|}$.

Step D. Let $W_0 \geq \|w(0)\|, S_{10} \geq |s_1(0)|$, and $S_{20} \geq |s_2(0)|$, and define $\bar{s}_1 = \sup_{t\geq 0}|s_1|$ and $\bar{s}_2 = \sup_{t \geq 0}|s_2|$. By combining (24) and (21), it can be written as

$$|\tilde{H}(s,w)| \leq F_0 + F_1(\bar{s}_1 + \bar{s}_2) \tag{82}$$

$$F_0 = H_0 + H_2W_0 \quad F_1 = H_1 + H_2\xi_1. \tag{83}$$

Assume temporarily that a constant H overestimating $|\tilde{H}(s,w)|$ for any $t \geq 0$ exists. Constants $\alpha_0, \ldots, \alpha_5$ can be found such that

$$\bar{s}_1 \leq S_{10} + \alpha_0 H\mu^2 + \alpha_1\mu + \frac{\alpha_2}{H} \tag{84}$$

$$\bar{s}_2 \leq S_{20} + \alpha_2 N\mu H + \sqrt{2(1-\beta)\alpha_3 H}\sqrt{\bar{s}_1} + \alpha_4 N\mu H. \tag{85}$$

Consider the inequality

$$H \geq F_0 + F_1\bar{s}_1(H) + F_1\bar{s}_2(H). \tag{86}$$

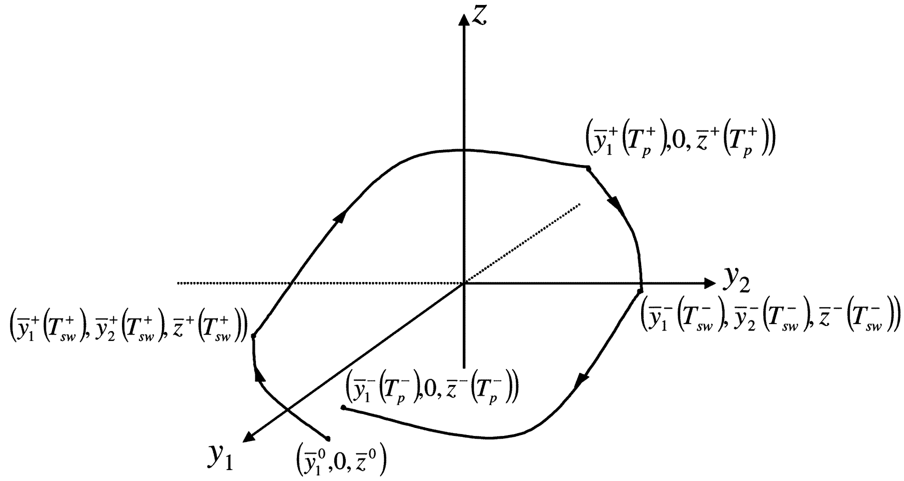

Fig. 13. Overall Poincaré map.

We will prove that (86) admits the semi-infinite solution interval $H \in (H^*, \infty)$. By simple manipulations, one can rewrite (86) as

$$H \geq \lambda_0 + F_1\alpha_0 H\mu^2 + F_1\alpha_1\mu + \frac{F_1\alpha_2}{G} + \lambda_1 H\mu + \lambda_2\sqrt{\alpha_2 + S_{10}H + \alpha_0 H^2\mu^2 + \alpha_1 H\mu} \quad (87)$$

where $\lambda_0, \ldots, \lambda_2$ are proper constants.

If the slope of the right-hand side of (87), viewed as a function of the variable H, is less than one for sufficiently large H, then the inequality (87) admits a semi-infinite solution interval of the type $H \in [H^*, \infty]$. Considering the higher order terms in H, one expresses such condition as

$$F_1\alpha_0\mu^2 + [\lambda_1 + \lambda_2\sqrt{\alpha_0}]\mu < 1 \quad (88)$$

yielding, in turns, $\mu \leq \mu^*$, where μ^* is the unique positive solution of equation $F_1\alpha_0\mu^{*2} + [\lambda_1 + \lambda_2\sqrt{\alpha_0}]\mu^* = 1$.

Step E. It has been demonstrated that

$$\mathcal{B}_1(\rho_1^*) = \{(s_1, s_2)\colon |s_1| \leq \rho_1^*\mu^2, s_2 = 0\} \quad (89)$$

is attracting. Consider the worst-case evolution starting from one of the neighbors (say the right one) of the attracting domain $\mathcal{B}_1$. The analysis performed in Step D can be applied by setting $S_{10} = \rho_1^*\mu^2$ and $S_{20} = 0$ in (84) and (85). By evaluating the corresponding values of $\bar{s}_1$ and $\bar{s}_2$ and considering the contraction condition (71), it can be concluded that there are ρ_1 and $\rho_2 > 0$ such that the following relationships will never be violated after the system has entered the set (89), and this concludes the proof

$$|s| \leq \rho_1\mu^2 \quad |\dot{s}| \leq \rho_2\mu. \quad (90)$$

Appendix II
Poincaré Map Derivation: General Procedure

Let us derive the Poincaré maps of the domain $y_1 > 0$, $f(w, y_1, 0, z_1) < 0$ on the surface $y_2 = 0$ into the domain $y_1 < 0$, $f(w, y_1, 0, z_1) > 0$ on the same surface $y_2 = 0$,generating by systems (34)–(36) and (37)–(38).

Let $y_1^0 > 0$ and denote as $w^+(\tau, \mu), y_1^+(\tau, \mu), y_2^+(\tau, \mu), z^+(\tau, \mu)$ and $\bar{y}_1^+(\tau, w), \bar{y}_2^+(\tau, w), \bar{z}^+(\tau, w)$ the solution of systems (34)–(36) and (37)–(38) with the initial conditions $w^+(0, \mu) = w^0, y_1^+(0, \mu) = y_1^0, y_2^+(0, \mu) = 0, z^+(0, \mu) = z^0 (w^0 \in W)$ and $\bar{y}_1^+(0, w) = \bar{y}_1^0, \bar{y}_2^+(0, w) = 0, \bar{z}^+(0, w) = \bar{z}^0$ such that $f(w, \bar{y}_1^0, 0, \bar{z}^0) < 0$ for all $w \in \bar{W}$.

Let T_{sw}^+ be the smallest positive root of the equation $\bar{y}_1^+(T_{sw}^+, w) = \beta\bar{y}_1^0$ and such that $(d\bar{y}_1^+/dt)(T_{sw}^+, w) = \bar{y}_2^+(T_{sw}^+, w) < 0$. From the implicit function theorem, there exists a switching time-instant

$$T_{\mu sw}^+(\mu) = T_{sw}^+ + O(\mu) \quad (91)$$

such that $y_1^+(T_{sw}^+(\mu), \mu) = \beta y_1^0, y_2^+(T_{sw}^+(\mu), \mu) < 0$.

Denote as $w_p^+(\tau, \mu), y_{1p}^+(\tau, \mu), y_{2p}^+(\tau, \mu), z_p^+(\tau, \mu)$, and $\bar{y}_{1p}^+(\tau, w), \bar{y}_{2p}^+(\tau, w), \bar{z}_p^+(\tau, w)$ the solutions of systems (35)–(36) and (37)–(38) with the initial conditions $w_p^+(T_{\mu sw}^+, \mu) = w^+(T_{\mu sw}^+, \mu), y_{1p}^+(T_{\mu sw}^+, \mu) = y_1^+(T_{\mu sw}^+, \mu), y_{2p}^+(T_{\mu sw}^+, \mu) = y_2^+(T_{\mu sw}^+, \mu)$, $z_p^+(T_{\mu sw}^+, \mu) = z^+(T_{\mu sw}^+, \mu)$ and $\bar{y}_{1p}^+(T_{\mu sw}^+, w) = \bar{y}_1^+(T_{\mu sw}^+, w), \bar{y}_{2p}^+(T_{\mu sw}^+, w) = \bar{y}_2^+(T_{\mu sw}^+, w), \bar{z}_p^+(T_{\mu sw}^+, w) = \bar{z}^+(T_{\mu sw}^+, w)$.

Let $T_p^+(w)$ be the smallest positive root of the equation $\bar{y}_{2p}^+(T_p^+(w), w) = 0$ and such that $(d\bar{y}_1^+/dt)(T_p^+, w) = \bar{y}_2^+(T_p^+, w) < 0$. From the implicit function theorem, one can conclude that there exists a switching time instant

$$T_{\mu p}^+ = T_p^+(w) + O(\mu) \quad (92)$$

such that $y_{2p}^+(T_{\mu p}^+, \mu) = 0, y_{1p}^+(T_{\mu p}^+, \mu) < 0$; so, we have designed the Poincaré maps

$$\Xi^+\left(w, \bar{y}_1^0, \bar{z}^0\right) = \begin{bmatrix} \bar{y}_{1p}^+(T_p^+(w), w) \\ \bar{z}_p^+(T_p^+(w), w) \end{bmatrix} \quad (93)$$

and

$$\Psi^+(w^0, y_1^0, z^0) = \begin{bmatrix} w_p^+(T_{\mu p}^+, \mu) \\ y_{1p}^+(T_{\mu p}^+, \mu) \\ z_p^+(T_{\mu p}^+, \mu) \end{bmatrix} = \begin{bmatrix} w^0 + O(\mu) \\ \Xi^+\left(w^0, y_1^0, z^0\right) + O(\mu) \end{bmatrix}. \quad (94)$$

Similarly, we can compute the Poincaré maps of the points $(\bar{y}_{1p}^{+}(T_p^{+}(w),w),\bar{z}_p^{+}(T_p^{+}(w),w))$ and $(w_p^{+}(T_{\mu p}^{+},\mu),$ $y_{1p}^{+}(T_{\mu p}^{+},\mu),z_p^{+}(T_{\mu p}^{+},\mu))$ of the domain $y_1 < 0$, $f(w,y_1,0,z_1)>0$ on the surface $y_2=0$ into the points

$$\Xi^{-}(w,\bar{y}_{1p}^{+}(T_p^{+}(w),w),\bar{z}_p^{+}(T_p^{+}(w),w)) = \begin{bmatrix}\bar{y}_{1p}^{-}(T_p^{-}(w),w)\\ \bar{z}_p^{-}(T_p^{-}(w),w)\end{bmatrix} \tag{95}$$

$$\Psi^{-}(w^0,y_1^0,z^0;\mu) = \begin{bmatrix} w_p^{-}(T_{\mu p}^{-},\mu)\\ y_{1p}^{-}(T_{\mu p}^{-},\mu)\\ z_p^{-}(T_{\mu p}^{-},\mu)\end{bmatrix} = \begin{bmatrix} w^0+O(\mu)\\ \bar{y}_{1p}^{-}(T_p^{-}(w^0),w^0)+O(\mu)\\ \bar{z}_p^{-}(T_p^{-}(w^0),w^0)+O(\mu)\end{bmatrix} \tag{96}$$

$$\bar{y}_{1p}^{-}(T_p^{-}(w^0),w^0)>0$$
$$f(w^0,\bar{y}_{1p}^{-}(T_p^{-}(w^0),w^0),0,\bar{z}_p^{-}(T_p^{-}(w^0),w^0))<0 \tag{97}$$

on the same surface $y_2 = 0$. Their detailed derivation is skipped for brevity. Combining them will provide for the overall Poincaré map (see Fig. 13), which allows checking the conditions for the existence and stability of the periodic limit cycles presented in Section IV.

Note that in conditions 1–4 the following notation is used: $T(w)=T_p^{-}(w),\bar{y}_1(T(w),w),\bar{y}_{1p}^{-}(T_p^{-}(w),w),\bar{z}(T(w),w)=\bar{z}_p^{-}(T_p^{-}(w),w)$, and $\Xi(w,\bar{y}_1^0,\bar{z}^0)=\Xi^{-}(w,\bar{y}_{1p}^{+}(T_p^{+}(w),w),\bar{z}_p^{+}(T_p^{+}(w),w))$.

Appendix III
Proof of Theorem 2

From the implicit function theorem, it follows that there exist some neighborhood $\mathcal{N}$ of the point $(w_0,\bar{y}_1^{*}(w_0),\bar{z}^{*}(w_0))$ and $\mu_0>0$ such that $\Psi\in\mathcal{C}[\mathcal{N}],\forall\mu\in[0,\mu_0]$.

Moreover, we can rewrite $\Psi(w,y_1,z,\mu)$ in the form

$$\Psi(w,y_1,z,\mu)=\begin{bmatrix} w+\mu Q(w,y_1,z,\mu)\\ R(w,y_1,z,\mu)\end{bmatrix} \tag{98}$$

where $Q(w,y_1,z,\mu)$ and $R(w,y_1,z,\mu)$ are sufficiently smooth functions such that

$$Q(w,\bar{y}_1^{*}(w),\bar{z}^{*}(w),0)=0, \tag{99}$$

$$R(w,\bar{y}_1^{*}(w),\bar{z}^{*}(w),0)=\Xi(w,\bar{y}_1^{*}(w),\bar{z}^{*}(w)) = (\bar{y}_1^{*}(w),\bar{z}^{*}(w)). \tag{100}$$

Let us rewrite the map Ψ in terms of the "error" variables $(\xi,\eta)=(y_1-\bar{y}_1^{*}(w),z-\bar{z}^{*}(w))$ yielding

$$\Psi(w,\xi,\eta;\mu) = \begin{bmatrix}\Psi_1(w,\xi,\eta,\mu)\\ \Psi_2(w,\xi,\eta,\mu)\end{bmatrix} = \begin{bmatrix} w+\mu Q(w,\xi+\bar{y}_1^{*}(w),\eta+z^{*}(w),\mu)\\ R(w,\xi+\bar{y}_1^{*}(w),\eta+z^{*}(w),\mu)-(\bar{y}_1^{*}(w),z^{*}(w))\end{bmatrix} \tag{101}$$

$$\Psi(w,0,0,0)=(w,0,0). \tag{102}$$

Existence of the periodic solution follows from the existence of the fixed point $(w^{*}(\mu),\xi^{*}(\mu),\eta^{*}(\mu))$ of the Poincaré map (101), which we are going to prove.

Existence conditions for the fixed point are written in the form

$$G(w^{*},\xi^{*},\eta^{*},\mu) = \begin{bmatrix} G_1(w^{*},\xi^{*},\eta^{*},\mu)\\ G_2(w^{*},\xi^{*},\eta^{*},\mu)\end{bmatrix} = \begin{bmatrix}\frac{1}{\mu}[w^{*}-\Psi_1(w^{*},\xi^{*},\eta^{*},\mu)]\\ (\xi^{*}\eta^{*})^T-\Psi_2(w^{*},\xi^{*},\eta^{*},\mu)\end{bmatrix}=0. \tag{103}$$

Taking into account that, if $\mu=0$, then $w^{*}(0)=w_0,\xi^{*}(0)=0,\eta^{*}(0)=0$ and $G_1(w_0,0,0,0)=-T_0(w_0)p(w_0)=0$, it turns out that if $\mu=0$, conditions in (103) are fulfilled. Moreover, taking into account that $G_2(w,0,0,0)=0,\forall w\in W$, we can conclude that $(\partial G_2/\partial w)(w_0,0,0,0)\equiv 0$.

Let us evaluate the Jacobian matrix of function G with respect to variables $w,(\xi,\eta)$ at $\mu=0$, and

$$\left.\frac{\partial G}{\partial(w,(\xi,\eta))}\right|_{(w_0,0,0,0)} = \begin{bmatrix}\tilde{G}_{11}(w_0) & \tilde{G}_{12}(w_0)\\ 0 & I_m-\tilde{G}_{22}(w_0)\end{bmatrix} \tag{104}$$

$$\tilde{G}_{11}(w_0) = -T_0(w_0)\frac{dp}{dw}(w_0)$$
$$\tilde{G}_{21}(w_0) = \frac{\partial G_2}{\partial(\xi,\eta)}(w_0,0,0,0)$$
$$\tilde{G}_{22}(w_0) = \frac{\partial\Xi}{\partial(y_1,z)}(w_0,\bar{y}_1^{*}(w_0),0,\bar{z}^{*}(w_0)) \tag{105}$$

is not degenerated. This means the map G admits an isolated fixed point $(w^{*}(\mu),\xi^{*}(\mu),\eta^{*}(\mu))$ corresponding to the periodic solution of systems (34)–(36) and (31)–(33), and $w^{*}(\mu)=w_0+O(\mu),y_1^{*}(\mu)=\bar{y}^{*}(w_0)+O(\mu),z^{*}(\mu)=\bar{z}^{*}(w_0)+O(\mu)$ □.

Appendix IV
Proof of Theorem 3

Denote as $\lambda_i(w_0),i=1,\ldots,m+1$ the eigenvalues of the matrix $(\partial\Xi/\partial(y_1,z))(w_0,\bar{y}_1^{*}(w_0),\bar{z}^{*}(w_0))$. Condition 5 now could be rewritten in the form $|\lambda_i(w_0)|<1,\forall i=1,\ldots,m+1$. The derivatives of Ψ with respect to variables $w,(\xi,\eta)$ read as

$$\left.\frac{\partial\Psi}{\partial(w,(\xi,\eta))}\right|_{(w_0,0,0,0)} = \begin{bmatrix} I_m+\tilde{\Psi}_{11}(w_0)+O(\mu) & \tilde{\Psi}_{12}(w_0)+O(\mu)\\ O(\mu) & \tilde{\Psi}_{22}(w_0)+O(\mu)\end{bmatrix} \tag{106}$$

$$\tilde{\Psi}_{11}(w_0) = \mu T_0(w_0)\frac{\partial p}{\partial w}(w_0)$$
$$\tilde{\Psi}_{21}(w_0) = \frac{\partial\Psi_1}{\partial(\xi,\eta)}(w_0,0,0,0)$$
$$\tilde{\Psi}_{22}(w_0) = \frac{\partial\Xi}{\partial(y_1,z)}(w_0,\bar{y}_1^{*}(w_0),0,\bar{z}^{*}(w_0)) \tag{107}$$

Then, in some vicinity of $(w_0, 0, 0, 0)$, $(\partial\Psi/\partial(w,\xi,\eta))$ has the two groups of eigenvalues

$$\begin{aligned} &1+\mu T_0(w_0)\nu_j(w_0)+\mu o(\mu), \qquad j=1,\ldots,n-2 \\ &\lambda_i(w_0)+O(\mu), \qquad i=1,\ldots,m. \end{aligned} \tag{108}$$

This means that under conditions 1–6 there exists some neighborhood of $(w_0, 0, 0, 0)$, where Ψ is a contraction map and the fast periodic solutions of systems (35)–(36) and (37)–(38) are orbitally asymptotically stable. □

Appendix V
Poincaré Map of System (46)

The solution of (46) with initial conditions $y_1(0) = y_1^0$, $y_2(0) = 0, z(0) = z^0$ is computed as follows. Let $t \in [0, T_{sw}^+]$, then

$$z(t) = (z^0+1)e^{-t} - 1 \tag{109}$$

$$y_2(t) = (z^0+1)(1-e^{-t}) - t \tag{110}$$

$$y_1(t) = y_1^0 + (z^0+1)(e^{-t}+t-1) - \frac{1}{2}t^2 \tag{111}$$

where $T_{sw}^+ = T_{sw}^+(y_1^0, z^0)$ is the smallest root of equation $y_1(T_{sw}^+) = (1/2)y_1^0$. Let $t \in [T_{sw}^+, T_p^+]$, then

$$z(t) = (z_{sw}^+ - 1)e^{-(t-T_{sw}^+)} + 1 \tag{112}$$

$$y_2(t) = y_{2_{sw}}^+ + (z_{sw}^+ - 1)(1-e^{-(t-T_{sw}^+)}) + t - T_{sw}^+ \tag{113}$$

$$y_1(t) = \frac{1}{2}y_1^0 + y_{2_{sw}}^+(t-T_{sw}^+) + (u_{sw}^+ - 1) \tag{114}$$

$$\cdot (t - T_{sw}^+ + e^{-(t-T_{sw}^+)} - 1) + \frac{1}{2}(t-T_{sw}^+)^2 \tag{115}$$

where $z_{sw}^+ = z(T_{sw}^+), y_{2_{sw}}^+ = y_2(T_{sw}^+), u_{sw}^+ = u(T_{sw}^+)$, and T_p^+ is the smallest root of equation $y_2(T_p^+) = 0$. System (46) is symmetric with respect to point $y_1 = y_2 = z = 0$, then the periodic solution parameters are determined by the (51).

Introduce the auxiliary variable $\Delta T^+ = T_p^+ - T_{sw}^+$, then the overall system results in

$$\begin{aligned} &\frac{1}{2}y_{1p}^0 + \left[\left(z_p^0+1\right)\left(1-e^{-\bar{T}_{sw}^+}\right) - \bar{T}_{sw}^+\right] \\ &\quad \cdot \Delta\bar{T}^+\left(\left(z_p^0+1\right)e^{-\bar{T}_{sw}^+} - 2\right) \\ &\quad \cdot \left(\Delta\bar{T}^+ + e^{-\Delta\bar{T}^+} - 1\right) + \frac{1}{2}\Delta\bar{T}^{+^2} = -y_{1p}^0 \end{aligned} \tag{116}$$

$$1 + \left(\left(z_p^0+1\right)e^{-\bar{T}_{sw}^+} - 2\right)e^{-\Delta\bar{T}^+} = -z_p^0 \tag{117}$$

$$\frac{1}{2}y_{1p}^0 + (z_p^0+1)(e^{-\bar{T}_{sw}^+} + \bar{T}_{sw}^+ - 1) - \frac{1}{2}\bar{T}_{sw}^{+^2} = 0 \tag{118}$$

$$\begin{aligned} &(z_p^0+1)(1-e^{-\bar{T}_{sw}^+}) + \left(\left(z_p^0+1\right)e^{-\bar{T}_{sw}^+} - 2\right)(1-e^{-\Delta\bar{T}^+}) \\ &\quad + \Delta\bar{T}^+ - \bar{T}_{sw}^+ = 0. \end{aligned} \tag{119}$$

The entries of matrix $\mathbf{J}$ can be computed by differentiating (48) with respect to y_1 and z, and evaluating the derivatives at the solution point (52). One obtains

$$\begin{aligned} \left.\frac{\partial \Xi_1^+}{\partial y_1}\right|_{(y_{1p}^0, z_p^0)} &= \frac{1}{2} - \bar{T}_{sw}^+ \left.\frac{\partial T_{sw}^+}{\partial y_1}\right|_{(y_{1p}^0, z_p^0)} \\ &\quad + \left(z_p^0 + 1 + \Delta\bar{T}^+ - \bar{T}_{sw}^+\right)\left.\frac{\partial \Delta T^+}{\partial y_1}\right|_{(y_{1p}^0, z_p^0)} \\ &\quad + \left(z_p^0+1\right)e^{-T_{sw}^+} + 2[e^{-\Delta\bar{T}^+} - 1] \\ &\quad - \left(\left.\frac{\partial T_{sw}^+}{\partial y_1}\right|_{(y_{1p}^0, z_p^0)} + \left.\frac{\partial \Delta T^+}{\partial y_1}\right|_{(y_{1p}^0, z_p^0)}\right) \\ &\quad \cdot \left(z_p^0+1\right)e^{-\bar{T}_{sw}^+ + \Delta\bar{T}^+} \end{aligned} \tag{120}$$

and similar expressions for the remaining derivatives $(\partial\Xi_1^+/\partial z)|_{(y_{1p}^0, z_p^0)}, (\partial\Xi_2^+/\partial y_1)|_{(y_{1p}^0, z_p^0)}, (\partial\Xi_2^+/\partial z)|_{(y_{1p}^0, z_p^0)}$, which are skipped for the sake of brevity. The partial derivatives of $T_{sw}^+(y_1, z)$ and $\Delta T^+(y_1, z)$ can be evaluated by differentiating (49) and (50). In particular, differentiating (49) with respect to y_1 yields $(1/2) - \bar{T}_{sw}^+(\partial T_{sw}^+/\partial y_1)|_{(y_{1p}^0, z_p^0)} + (z_p^0 + 1)(1 - e^{-\bar{T}_{sw}^+})(\partial T_{sw}^+/\partial y_1)|_{(y_{1p}^0, z_p^0)} = 0$, from which it is easy to derive that $(\partial T_{sw}^+/\partial y_1)|_{(y_{1p}^0, z_p^0)} = (1/2/\bar{T}_{sw}^+ - (z_p^0+1)(1-e^{-T_{sw}^+})) = 0.2529$. The remaining entries of the Jacobian matrix (54) can be derived similarly.

Acknowledgment

The authors would like to thank the Associate Editor Prof. Celikovsky for his comments that improved the paper.

References

[1] D. V. Anosov, "On stability of equilibrium points of relay systems," *Automatica i telemechanica (Autom. Remote Control)*, vol. 20, no. 2, pp. 135–149, 1959.

[2] D. P. Atherton, *Nonlinear Control Engineering: Describing Function Analysis and Design*. London, U.K.: Van Nostrand Reinhold, 1975.

[3] J. Andre and P. Seibert, "Uber die stuckweise linearen differential Gleichungen, die bei Regelungsproblemen auftreten," *Arch. Math.*, vol. 7, no. 3, pp. 148–164, 1956.

[4] G. Bartolini, A. Ferrara, and E. Usai, "Chattering avoidance by second order sliding mode control," *IEEE Trans. Autom. Control*, vol. 43, no. 2, pp. 241–246, Feb. 1998.

[5] G. Bartolini, A. Ferrara, A. Levant, and E. Usai, "On second order sliding mode controllers," in *Lecture Notes in Control and Information Sciences*, K. D. Young and U. Ozguner, Eds. Berlin, Germany: Springer-Verlag, 1999, vol. 247, Variable Structure Systems, Sliding Mode and Nonlinear Control, pp. 329–350.

[6] G. Bartolini, A. Ferrara, A. Pisano, and E. Usai, "On the convergence properties of a 2-sliding control algorithm for nonlinear uncertain systems," *Int. J. Control*, vol. 74, pp. 718–731, 2001.

[7] G. Bartolini, A. Pisano, E. Punta, and E. Usai, "A survey of applications of second order sliding mode control to mechanical systems," *Int. J. Control*, vol. 76, no. 9/10, pp. 875–892, 2003.

[8] D. Benmerzouk and J. P. Barbot, "Lyapunov-Schmidt method dedicated to the observer analysis and design," *Math. Problems Eng.*, pp. 1–28, 2006, Article ID 43681.

[9] I. Boiko, "Analysis of sliding modes in the frequency domain," *Int. J. Control*, vol. 78, no. 13, pp. 969–981, 2005.

[10] I. Boiko, L. Fridman, and M. I. Castellanos, "Analysis of second order sliding mode algorithms in the frequency domain," *IEEE Trans. Autom. Control*, vol. 49, no. 6, pp. 946–950, Jun. 2004.

[11] I. Boiko and L. Fridman, "Analysis of chattering in continuous sliding-mode controllers," *IEEE Trans. Autom. Control*, vol. 50, no. 9, pp. 1442–1446, Sep. 2005.

[12] I. Boiko, L. Fridman, R. Iriarte, A. Pisano, and E. Usai, "Parameter tuning of second-order sliding mode controllers for linear plants with dynamic actuators," *Automatica*, vol. 42, no. 5, pp. 833–839, May 2006.

[13] A. G. Bondarev, S. A. Bondarev, N. Y. Kostylyeva, and V. I. Utkin, "Sliding modes in systems with asymptotic state observers," *Automatica i telemechanica (Autom. Remote Control)*, vol. 46, no. 5, pp. 679–684, 1985.

[14] J. A. Burton and A. S. I. Zinober, "Continuous approximation of VSC," *Int. J. Syst. Sci.*, vol. 17, pp. 875–885, 1986.

[15] S. Celikovsky, "Global linearization of nonlinear systems—A survey," *Banach Center Pubs.*, vol. 32, pp. 123–137, 1995.

[16] M. Di Bernardo, K. H. Johansson, and F. Vasca, "Self-oscillations and sliding in relay feedback systems: Symmetry and bifurcations," *Int. J. Bifurcation Chaos*, vol. 11, pp. 1121–1140, Apr. 2001.

[17] C. Edwards and S. K. Spurgeon, *Sliding Mode Control*. London, U.K.: Taylor & Francis, 1998.

[18] S. V. Emlyanov, S. K. Korovin, A. Levantovsky, and A. Levant, "Higher order sliding modes in the binary control systems," *Soviet Phys., Doklady*, vol. 31, pp. 291–293, 1986.

[19] A. F. Filippov, *Differential Equations with Discontinuous Right-Hand Sides*. Dordrecht, The Netherlands: Kluwer, 1988, Mathematics and Its Applications.

[20] L. Fridman, "An averaging approach to chattering," *IEEE Trans. Autom. Control*, vol. 46, no. 8, pp. 1260–1264, Aug. 2001.

[21] L. Fridman, "Singularly perturbed analysis of chattering in relay control systems," *IEEE Trans. Autom. Control*, vol. 47, no. 12, pp. 2079–2084, Dec. 2002.

[22] L. Fridman, "Chattering analysis in sliding mode systems with inertial sensors," *Int. J. Control*, vol. 76, no. 9/10, pp. 906–912, 2003.

[23] T. Floquet, J.-P. Barbot, and W. Perruquetti, "Higher-order sliding mode stabilization for a class of nonholonomic perturbed systems," *Automatica*, vol. 39, pp. 1077–1083, 2003.

[24] A. Isidori, *Nonlinear Control Systems*, 3rd ed. Berlin, Germany: Springer-Verlag, 1995.

[25] U. Itkis, *Control Systems of Variable Structure*. NewYork: Wiley, 1976.

[26] A. Levant, "Sliding order and sliding accuracy in sliding mode control," *Int. J. Control*, vol. 58, pp. 1247–1263, 1993.

[27] A. Levant, "Higher order sliding modes, differentiation and output-feedback control," *Int. J. Control*, vol. 76, no. 9/10, pp. 924–941, 2003.

[28] D. Liberzon, *Switching in Systems and Control*. Boston, MA: Birkhauser, 2003.

[29] P. Nistri, "A note on the approximability property of nonlinear variable structure systems," in *Proc. IEEE 28th Conf. Decision Control*, 1989, pp. 815–818.

[30] Y. Orlov, L. Aguilar, and J. C. Cadiou, "Switched chattering control vs. backlash/friction phenomena in electrical servo-motors," *Int. J. Control*, vol. 76, no. 9/10, pp. 959–967, 2003.

[31] Y. I. Neimark, "About periodic solutions of relay systems," in *Memorize of A.A. Andronov* (in Russian). Moscow, Russia: Nauka, 1973, pp. 242–273.

[32] L. S. Pontriagin and L. V. Rodygin, "Periodic solution of one system of differential equation with small parameter near the derivative," (in Russian) *Doklady Academii Nauk*, vol. 132, pp. 537–540, 1960.

[33] Y. B. Shtessel and L. Young-Ju, "New approach to chattering analysis in systems with sliding modes," in *Proc. IEEE Conf. Decision Control*, 1996, vol. 4, pp. 4014–4019.

[34] Y. B. Shtessel, I. A. Shkolnikov, and M. D. J. Brown, "An asymptotic second-order smooth sliding mode control," *Asian J. Control*, vol. 5, no. 4, pp. 498–5043, 2003.

[35] E. Sontag, *Mathematical Control Theory*. New York: Springer-Verlag, 1998.

[36] J. J. Slotine and W. Li, *Applied Nonlinear Control*. Englewood Cliffs, NJ: Prentice-Hall, 1991.

[37] A. Tikhonov, "Systems of differential equations containing a small parameter in the derivatives," (in Russian) *Mat. Sbornik*, vol. 31, no. 73, pp. 575–586, 1952.

[38] V. I. Utkin, "Variable structure systems with sliding modes: A survey," *IEEE Trans. Autom. Control*, vol. AC-22, no. 2, pp. 212–222, Apr. 1977.

[39] V. I. Utkin, *Sliding Modes and Their Application in Variable Structure Systems*. Moscow, Russia: Mir Publishers, 1978.

[40] V. I. Utkin, *Sliding Modes in Control and Optimization*. Berlin, Germany: Springer-Verlag, 1992.

[41] V. Utkin, J. Guldner, and J. Shi, *Sliding Modes in Electromechanical Systems*. London, U.K.: Taylor & Francis, 1999.

[42] V. I. Utkin, "First Stage of VSS: people and events," in *Lecture Notes in Control and Information Science*, X. Yu and J.-X. Xu, Eds. London, U.K.: Springer-Verlag, 2002, vol. 274, Variable Structure Systems: Towards the 21st Century, pp. 1–33.

[43] Y. Z. Tsypkin, *Relay Control Systems*. Cambridge, U.K.: Cambridge Univ. Press, 1984.

[44] K. D. Young, V. I. Utkin, and U. Ozguner, "A control engineer's guide to sliding mode control," *IEEE Trans. Control Syst. Technol.*, vol. 7, no. 3, pp. 328–342, May 1999.

[45] K. K. Zhilcov, *Approximate Methods of Variable Structure Systems Analysis* (in Russian). Moscow, Russia: Nauka, 1974.

[46] T. Zolezzi, "A variational approach to second-order approximability of sliding mode control system," *Optimization*, vol. 53, pp. 641–654, 2004.

Igor Boiko (M'94–SM'04) was born in Russia. He received the M.S. degree in electromechanical engineering and the Ph.D. degree in control engineering both from Tula State University, Tula, Russia, in 1984 and 1990, respectively.

He was a Senior Research Scientist at Tula State University and conducted a number of successful researches for the Russian aerospace industry. Since 1998 he has been working as a Process Control Engineer and Consultant in the petrochemical industry in Canada. He worked for such companies as SNC-Lavalin, Honeywell, ChevronTexaco, Syncrude. He played a leading role in the control logistics and distributed control system (DCS) design and configuration on Syncrude UE-1 Project—one of the biggest projects in the Canadian history. Currently, he is an Adjunct Professor at the University of Calgary, Calgary, ON, Canada. He has authored over 70 papers and is the holder of two patents. His research interests include frequency-domain methods of analysis and design of nonlinear systems and sliding-mode control systems, in particular, process control theory and applications.

Dr. Boiko is a Professional Engineer registered in Alberta, Canada.

Leonid Fridman (M'96) received the M.S. degree in mathematics from Kuibyshev (Samara) State University, Samara, Russia, the Ph.D. degree in applied mathematics from Institute of Control Science, Moscow, Russia, and Doctor of Science degrees in control science from Moscow State University of Mathematics and Electronics, Moscow, Russia, in 1976, 1988, and 1998, respectively.

In 1976–1999, he was with the Department of Mathematics, Samara State Architecture and Civil Engineering Academy, Samara, Russia. In 2000–2002, he is with the Department of Postgraduate Study and Investigations, Chihuahua Institute of Technology, Chihuahua, Mexico. In 2002, he joined the Department of Control, Division of Electrical Engineering of Engineering Faculty, National Autonomous University of Mexico (UNAM), Mexico. He is an editor of two books and four special issues on sliding-mode control. He published over 160 technical papers. His research interests include variable structure systems and singular perturbations.

Dr. Fridman is an Associate Editor of the Conference Editorial Board of IEEE Control Systems Society and Member of Technical Committee on Variable Structure Systems and Sliding-Mode Control of the IEEE Control Systems Society.

Alessandro Pisano (M'07) was born in Sassari, Italy, in 1972. He graduated in electronic engineering in 1997 and received the Ph.D. degree in electronics and computer science in 2000 from the Department of Electrical and Electronic Engineering (DIEE), Cagliari University, Cagliari, Italy.

Currently, he is a Research Associate at DIEE. His current research interest include the theory and application of nonlinear and robust control, with special emphasis on sliding-mode control design and implementation, robotics, and power plants simulation and control. He has authored over 70 papers, and is the holder of one patent in the field of underwater robotics.

Dr. Pisano is an Associate Editor of the Conference Editorial Board of the IEEE Control Systems Society. He served as Chair of the National Organizing Committee and Program Committee Member for the Ninth IEEE International Workshop on Variable Structure Systems, Alghero, Italy, June 2006. He is a Professional Engineer registered in Cagliari, Italy.

Elio Usai (M'97) was born in Sassari, Italy, in 1960. He graduated in electrical engineering from the University of Cagliari, Cagliari, Italy, in 1985.

Until 1994, he has been working for international industrial companies. Since 1994 he has been at the Department of Electrical and Electronic Engineering (DIEE), University of Cagliari, where he is currently an Associate Professor of Automatic Control. His current research interests are in the field of control engineering, variable structure systems, and control of mechanical systems.